Escola de Camins
Escola Tècnica Superior d'Enginyeria de Camins, Canals i Ports
UPC BARCELONATECH

TREBALL FINAL MÀSTER

Application of hydrodynamics' analytical models in estuaries and submarine springs for the quantification of fresh groundwater discharge to the sea

Treball realitzat per:
Foncillas Osorio, Daniel

Dirigit per:
Espino Infantes, Manuel
Folch Sancho, Albert
Fernàndez-Garcia, Daniel

Màster en:
Enginyeria de Camins, Canals i Ports

Barcelona, juny 2021

Departament d'Enginyeria Civil i Ambiental

AKNOWLEDGMENTS

I would like to thank all the people who in one way or another have been part of this work at some point in its development. Finishing this Final Project does not mean only the end of one simple project, but rather the success of the career and the master, so I would also like to thank all those who have lived with me over the years.

First of all, I would like to thank Manuel Espino, Albert Folch and Daniel Fernàndez, the advisors of my Final Project, especially to Manuel, who gave me the opportunity to carry it out. From the original idea to the final moment, they have always been present and have helped me in the day to day and in creating, little by little, what now is the present project. In addition, I am grateful for all the time they have invested, from all the meetings that have been held, which have not been few, to all the time that has been spent in reading and correcting. From the three of them I have learned so much all these months.

Secondly, during all the years of the career you meet many people but, in the end, the ones you get to know can be counted on the fingers of one hand. I would like to thank the three people I have taken with me on this great journey: Blanca, Ana and Paula. Blanca, you know that without you nothing would have been the same. You have been a pillar on which I have always been able to rely on throughout my university years, including my Erasmus experience.

Finally, yet importantly, to my parents Joan and Alicia, and to my sisters Alba, Alicia and Marta, who live day by day with me, giving me advice and they always cheer me up. They are all examples of effort, perseverance and have always been supportive through all my life. Above all, I want to thank the most special person in my life, Victoria, because at the end you are the one who trusts me the most and is always there to help me from the very beginning to end.

ABSTRACT

Nowadays, as it is commonly said, world is in a critical situation, where climate change and land over-exploitation produce negative environmental effects, such as increase of the sea level and subsequent intrusion of saltwater in coastal aquifers, among others. The last one, despite being a natural process, in recent years has increased its importance as a result of anthropogenic activities.

Many scientific studies look after a better understanding of the aforementioned Sea Water Intrusion, the interface between fresh and salt water occurring in coastal aquifers or the Submarine Groundwater Discharge from these aquifers to the ocean. The present study focuses mainly on the last one, comparing the SGD process to submarine outfall discharge to try then calculating the Fresh SGD (FSGD) fluxes in alternative ways.

These upwelling fluxes can be calculated by approaching and adapting two different methodologies for FSGD flux calculation used in the studied upwellings; one related to the methodology and formulation behind the submarine outfalls to dump wastewater to the sea ('Submarine Diffuser Model') and the other related to the so called 'Box Model' methodology, based on salinity and temperature balance condition when a different water mass outcrops in the ocean. With these models, we wanted to test some methodologies with different degrees of complexity.

To contrast the results, three different data scenarios are considered, two in a same site (at Torre Badum, Castellón) but at different seasons of the year, and the other in a completely different aquifer with other characteristics (at Kahauloa Bay, Hawaii).

Once all the methodologies are deeply studied and the calculus are done, a general evaluation of the results has been made, and the feasibility to use the proposed models has been analyzed. The principal conclusions of the project are the following:

1) The submarine outfall methodology, the most complex one, is not suitable to be applied in the resolution of these flow problems of an FSGD. None of the considerations taken for the adaptation of such a method is technically valid, and the obtained results are far from being optimistic.
2) As for the box model, the 'complex' variant for this second methodology was discarded at the outset, because it 'broke down' for some reasons and is not a proper methodology to use for FSGD flux estimation.
3) Finally, opposed to the rest, the 'simple' box model has passed the tests and, with a certain instability on its accuracy level, it is a relatively good approximation as a new methodology that has never been tested in a context such as this (its average balance of the overall project remains at an accuracy of 102%), much cheaper and easy to apply than most current methodologies usually applied.

This conclusions let us to think that a new possibility is raised for the FSGD fluxes calculation, offering advantages over the current measurements using radioactive Radium and Radon tracers, much more expensive and complex processes than standard measurements in oceanography that are needed to carry on the proposed 'Box Model' methodology, such as data

collection for temperature or salinity profiles. Therefore, the application of few scenarios does not give an excellent calibration level, but the numbers indicate a very promising potential, and it should be noticed that, in order to implement the simplest method, the data required is very accessible making it an easy and cost-effective method to apply on future FSGD quantification processes.

TABLE OF CONTENTS

LIST OF FIGURES

LIST OF TABLES

1. INTRODUCTION

In coastal aquifers, the phenomenon of mixing of continental freshwater and seawater occurs. They are usually formed by different types of sediment or rock, tending to have a low permeability, in which water flows through cracks and fractures or between their inter-particle's voids (karstified limestone, fractured rock or unconsolidated sands). Such water flow is mainly due to hydraulic gradient, but density gradients, related to water salinity, also affect these body masses movements on a lower scale.

The increasing demand for freshwater, especially in coastal areas where the population is growing significantly, the alteration of natural hydrological conditions, climate change and groundwater contamination will increase the pressure on available water resources and the valuable ecosystems that depend on them. Besides their natural values, coastal aquifers are key, valuable, and important natural infrastructures for water supply (Custodio, 2005).

Not only does this high demand apply extreme pressure on groundwater resources, but also they are threatened by the disposal of waste and sewage and leaching of contaminants. These problems are specially critic in arid or semi-arid areas where groundwater is the only source of fresh water and the periods of lowest freshwater recharge for the aquifer coincide with periods with highest demand. Although this problem exists in any aquifer, the risk in coastal aquifers is much greater due to the possibility of marine intrusion (Figure 1), as an overexploitation consequence, and the inability to supply large communities with the necessary and sufficient fresh water.

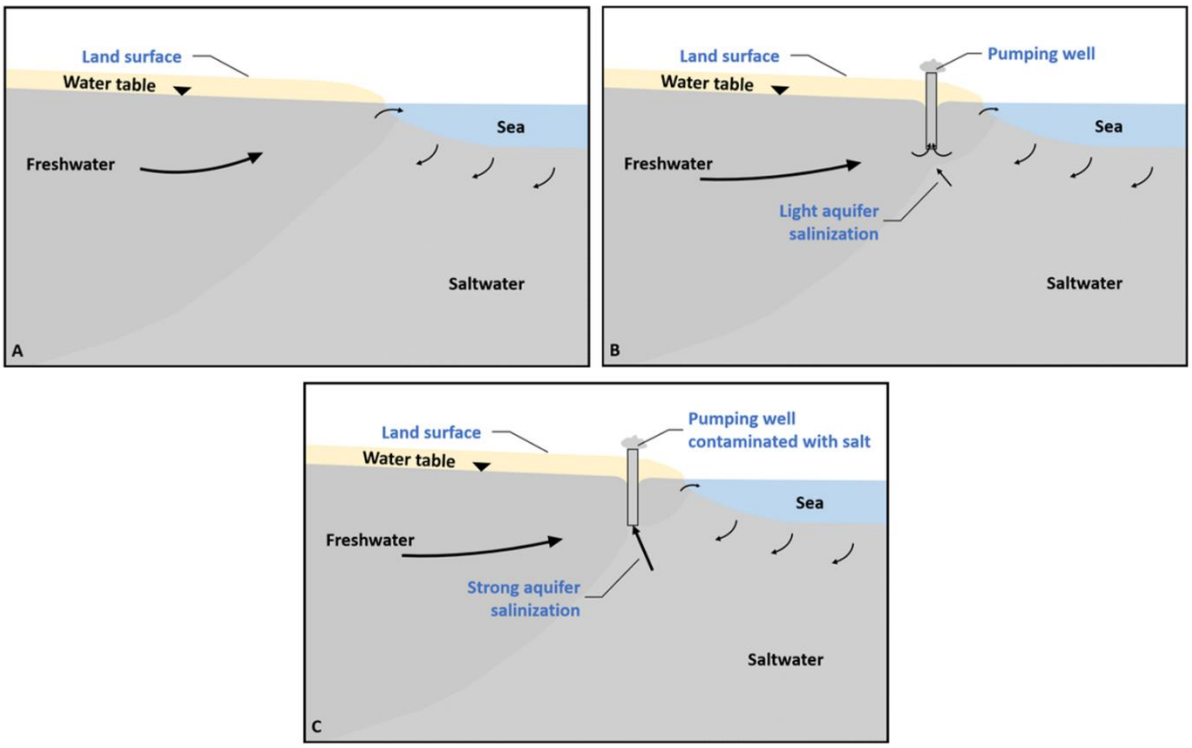

Figure 1. Process of the aquifer salinization by intrusion of the saltwater, modified from (Kalakan, 2018)

From a water management point of view, the fact that coastal aquifers are highly vulnerable to saltwater intrusion is truly a global phenomenon, resulting in one of the huge risks that humans are now facing. Moreover, the current state is not good at all and aggravation of the problem of fresh groundwater salinization through seawater outcrop is expected in the next decades due to population and economic growth, deterioration of water quality by pollution, reduced infiltration capacity as a result of urbanization, declining river discharge and climate change (Post, 2005).

On the other hand, Submarine Groundwater Discharge ('SGD') is a global, naturally occurring process that happens where coastal aquifers has direct communication with the sea (Moore, 1999). It can be defined as the water mass that flows through a coastal aquifer and ends pouring into the surrounding marine environment, encompassing both freshwater (FSGD) and recirculated ocean saltwater through shore seabed. Interest in researching about SGD has increased over the past two decades. This is probably because of the implications that the discharging groundwater has in marine environments and ecosystems, and in the exchange of fluxes at the freshwater-saltwater interface of coastal aquifers. For this reason, the trend is to adopt broader and multidisciplinary approaches for coastal aquifers' investigation (Taniguchi et al., 2019)

However, being the SGD water properties that differ from the ocean saltwater invisible and imperceptible to the human eye in plain light (salinity, temperature, nutrients…) and, knowing that submarine groundwater discharges are not temporally and spatially constant, locating and identifying underwater freshwater upwellings is not an easy task for researchers and their studies. Thus, the real challenge here starts from the very beginning (Kelly et al., 2013).

Nowadays, the sample of radionuclide isotope tracers is a process very used (the most) to study the location and properties of SGD over small-medium scale. But there can be some interesting alternatives to that method. For example, there is a similitude relation between submarine groundwater discharge emerging from coastal aquifers and submarine outfalls waste discharge. On the other hand, SGD zones undergo some process similar to what is defined as an estuary (defined in section 2.1), and that's the reason why SDG zones could be called "submarine estuaries".

With these two ideas in mind, two different methods to obtain FSGD fluxes will be proposed and explained in detail in this work.

2. STATE OF ART

2.1. Coastal aquifers and Submarine Groundwater Discharges

2.1.1. Coastal aquifers

Aquifers can be defined as (Todd, 1959) does, by its Latin meaning. He states that aquifer comes from two Latin parts: *aqui-* comes from "*aqua*" which means *water*, and *-fer* comes from "*ferre*" which means *to hold* or *to bear*. In this way, an aquifer can be defined as a fully saturated geological porous media containing water which allows it to move through its void cavities in ordinary field conditions. In other words, a geological porous formation that storages water but is not able to transfer water to other surrounding formations won't be referred as an aquifer.

Coastal aquifers are those aquifers where fresh groundwater from continental drainage meets seawater (Figure 2), being different from other type of aquifers by this maritime hydraulic connection. In other words, we can define coastal aquifers as the subsoil equivalents of coastal areas, where inland groundwater and seawater are found (Post, 2005).

The sea connection that coastal aquifers have, gives them a set of peculiarities which render coastal aquifers a complexity that is far from being completely understood.

These aquifers are vulnerable to the salinization of fresh groundwater due to the interaction that is fostered with the intrusion of seawater. Its vulnerability is so critical due to the enormous responsibility they have in sustaining coastal and marine ecosystems, such as coastal lagoons or shallow marine environments (Taniguchi et al., 2019). These environments depend on fresh groundwater contribution to equilibrate fresh and saline conditions.

Their importance and value do not only affect the ecosystems connected to them, but also the population whose activity and prosperity is directly related to the demand for fresh water it requires. According to (Jiao and Post, 2019) population density in coastal areas is way bigger in comparison to population density in inland areas. Data reveal that a little bit less than a fifty percent of the world's population, this is almost 3,9 billion people, live in coastal areas or near them (ocean is at maximum 100 km away) (Post, 2005). Obviously, the bigger the population density is, the higher the economic activity and progress are (coastal zones generate more or less 28 trillion dollars to contribute to global economy) (IOC-UNESCO and UNEP, 2016), and also higher the freshwater demand is. A common way to obtain that amount of water is to take it from the provided by groundwater in those zones. This makes coastal aquifers an essential asset for global economy.

The future does not look too bright, as the rising demand for fresh groundwater, disruption and uncontrolled natural hydrological conditions, acceleration of climate change and more common groundwater contamination will increase demand on available water letting the situation about natural resources and valuable ecosystems become very tense and out of control.

Proper management requires sufficient knowledge and understanding of the coastal groundwater processes. Nowadays, despite the large amount of research in the field of coastal

hydrogeology, there is still plenty of room for improvement, as in the knowledge gaps of systematic data collection or understanding the interface between the fresh and saltwater (Michael et al., 2017). The vast majority of studies that can be seen today as scientific literature focus in two single topics: the aforementioned interface between saltwater and freshwater in aquifers, constantly affected by Sea Water Intrusion or 'SWI', (most commonly studied by hydrogeologists from an onshore point of view to quantify and qualify the state of the aquifer's freshwater body) and the discharge of groundwater to the sea (most commonly studied by oceanographers to quantify the Submarine Groundwater Discharge, the '*SGD*').

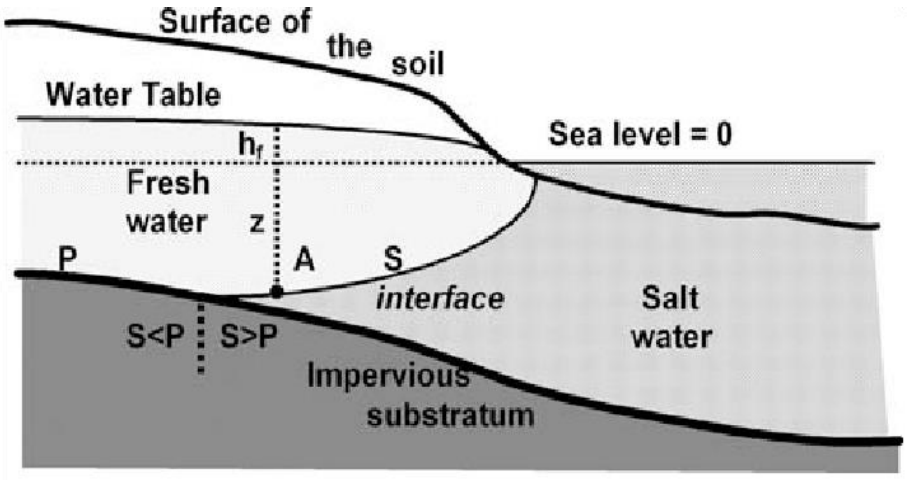

Figure 2. Scheme of coastal aquifer (Padilla, 2007)

2.1.2. Submarine Groundwater Discharges

As previously said, Submarine Groundwater Discharge ('*SGD*') is a worldwide ocean process that occurs in zones where coastal aquifers connects with the sea.

SGD can be defined as the water mass that flows through the geological porous formation, which forms a coastal aquifer with scale of meters to kilometers, and ends pouring into the surrounding marine environment. All this water body encompasses both freshwater coming from terrestrial surface percolation (drainage of coastal meteoric water or drainage from other inland aquifers) and recirculated ocean saltwater through shore seabed (Figure 3). Unlike runoff water discharge, there is relatively little information and studies about submarine groundwater discharge (Varma *et al.*, 2010 and Moore, 2010). Even so, interest in SGD has been continuously increasing since the end of 20th century, because of the effect that SGD has on many environmental issues.

Several SGD studies and researches done in punctual coastal areas reveal that the amount of nutrients directly discharged to the sea from rivers and surface runoff in regional areas is equivalent, by and large, to a sixty three percent of the amount of nutrients that groundwater pours to the ocean through coastal aquifers by SGD in few coastline kilometers (order of tens) (Smith et al., 2003, Johnson *et al.*, 2008 and Cho *et al.*, 2018). What is more, not only in terms

of nutrients but also in terms of volume, (Capone and Bautista, 1985) discovered that in the Great South Bay in New York, where they did some SGD studies, up to the 60% of the influx to the ocean was through coastal aquifers by SGD processes. After them, the scientific community has also studied the new paradigm and confirmed the same result in different locations all around the world.

In the vast majority of cases, SGD water is less saline than the ocean saltwater, and its temperature usually differs from sea water receiving the discharge being either colder or warmer. As it is less dense, SGD usually flows upwards forming a buoyant plume that begins near coastline and extends out to sea (Kelly *et al.*, 2013).

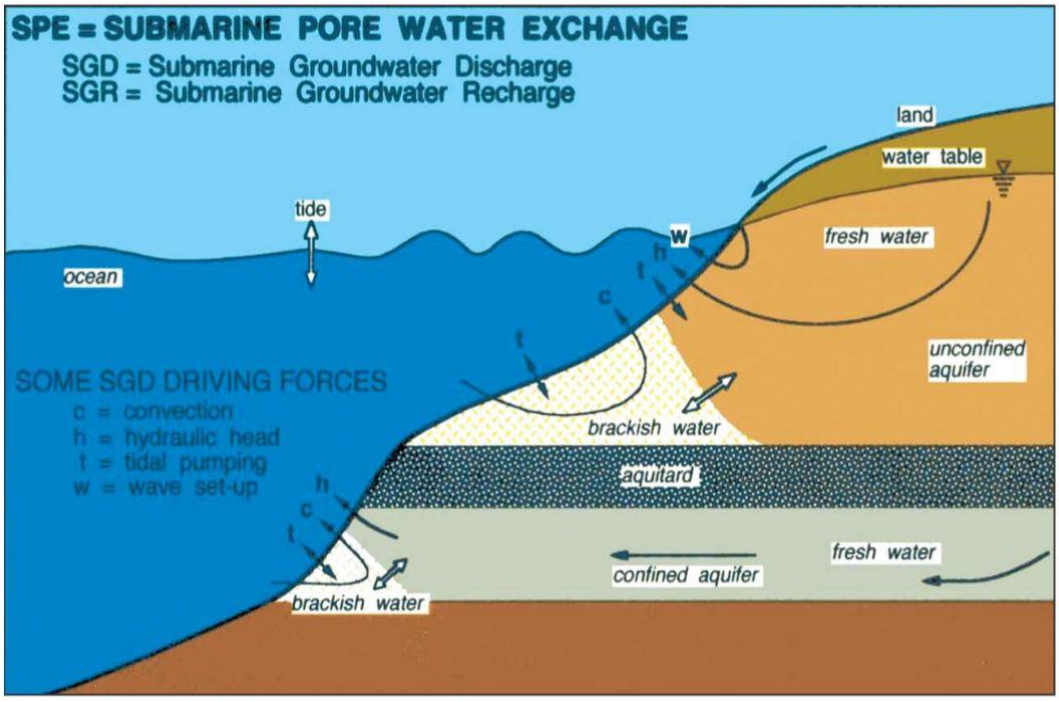

Figure 3. Schematic picture of processes associated with SGD where arrows indicate water movement (Kumar, 2010)

2.2. Current SGD studies using TIR, Ra and Rn tracers

As mentioned in section 1, the identification of SGDs is a tough process due to the constant change of form and dimensions of the plume, as well as the key properties that identifies SGDs are imperceptible for the human eye.

To address the issue, scientists generally rely on a multitude of traditional land-based methodologies, such as geochemical tracers (Radon and Radium), salinity, piezometers, temperature, etc. Combining both airborne Thermal Infrared (TIR) overflights and shoreline radionuclide surveys it is possible to detect, qualify and quantify submarine groundwater discharge (Tamborski *et al.*, 2015 and Kelly *et al.*, 2013). For example, with this combination of methodologies, (Mejías et al., 2012) were able to identify multiple point-source plumes of SGD along Spanish eastern coast that would have not been identified from satellite imagery alone.

On one hand, Thermal Infrared (TIR) remote sensing can resolve the spatial and temporal variation of groundwater discharge along a shoreline in the top-most surface of a water body (Figure 4). Fresher and more buoyant SGD water will rise above already present saline seawaters. For instance, FSGD usually exists at the average annual groundwater temperature that differs from the ocean surface-water temperature. This means that the SGD tends to leave his own distinct thermal signature (Anderson, 2005), making detection of SGD via Thermal Infrared remote sensing possible in environments where the receiving surface-water body has thermal contrast with the discharging pore fluid (Tamborski *et al.*, 2015). Infrared technology is commonly used at large scales via images taken by satellite (having pixels resolutions between 60 meters to tens of kilometers), inexpensive available to all users who only need broad views of SGD. However, it can also be used at smaller scales as via aircraft, which are suitable for more detailed SGD characterization (having pixel resolutions in an order of approximately 5 meters or less, depending on the flight altitude adjustments). This type of data collection, although allows to see little and individual discharges with their common small localized features, it is way more expensive than the first one, involving costs for the aircraft time and the hardware needed to process data. In the last decades, lots of studies have been carried away with thermal detection of plumes to study SGD. Collectively, these studies demonstrate the general utility and applicability of aerial infrared thermography to a wide variety of settings (Kelly *et al.*, 2013).

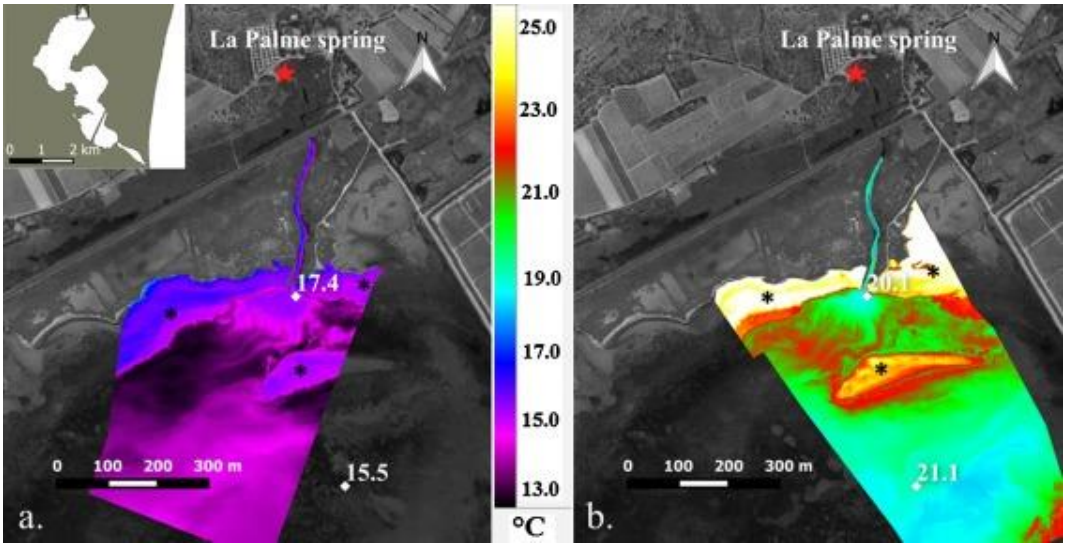

Figure 4. Example of an airborne TIR imagery survey in France (20/9/2012 at a) 9:26 and b) 16:55) (Bejannin, 2017)

On the other hand, both Radon and Radium are often used as radionuclide tracers to study SGD in regional scale zones. Radon (^{222}Rn) and radium (^{223,224}Ra) isotopes are perfect agents to quantify SGD fluxes because they have short half-lives and are naturally elevated in groundwater by several orders of magnitude relative to surface-waters (Tamborski *et al.*, 2015). As it has just been said, their quite short half-lifetimes (^{222}Rn has a $T_{1/2}$ = 3,8 days; ^{224}Ra has a $T_{1/2}$ = 3,6 days; ^{223}Ra has a $T_{1/2}$ = 11,4 days), make these three isotopes become enough widely functional to be useful for both tracking submarine groundwater discharge fluxes, by in-situ measurements taken along the plume location, and also estimating the apparent water ages (Moore, 2000). For instance, to carry out ^{224}Ra isotope measurement, water samples are taken at different study points homogeneously distributed throughout the area in which the TIR identifies the presence

of an underwater upwelling (a total of twenty or fifty liters of water are collected), filtering them through acrylic fibers impregnated with manganese (IV) oxide (MnO_2) with a very low filtering velocity (< 1 l/min), and then take these fibers to be analyzed in the laboratory using a radium delayed coincidence process by a counter (RaDeCC) (Moore, 2000).

As a summary, it has been shown by many scientific articles and studies that sampling radionuclide isotope tracers coupled with Thermal Infrared surveys are profitable to identify, qualify and quantify SGD over small-medium scale (Peterson et al., 2009, Mejías et al., 2012, Tamborski *et al.*, 2015). But even more interesting is the fact that there are some alternatives to obtain FSGD flows which can offer some pros and cons:

- The way an SGD behaves when emerging in the ocean is very similar to the way that submarine outfalls work for discharging treated waters to the open sea; both processes concern the existence of a 'plume' of water with non-identical properties (commonly with temperature and salinity differences) that emerges from submarine depths to the sea surface and then expands through mixing processes until both waters dilute with each other.
- An estuary can be defined as the places where continents and oceans meet, or where rivers meet seas. These zones have huge potential as ecosystems with good environmental conditions, since freshwater collected over vast regions of the land pours into an ocean, which sends saltwater upstream far beyond the river mouth, creating perfect conditions by vigorous mixing between the two fluids. (Tomczak, 1996). For this reason, SGD zones could be call "submarine estuaries".

In the following subsections, two different methods to obtain FSGD fluxes will be proposed and explained in detail.

2.3. Method nº1: Submarine Outfalls – 'Submarine Diffuser Model' methodology

Residuals from the land have always been dragged by fresh groundwater, runoff water or by rivers and, in the majority of cases, released to the ocean. Thus, ocean is a global sink for all land wastes. At first, this process was part of a natural thing but through ages has been transformed to something more anthropic. As Fischer *et al.*, (1979) say, the problem is that human need to be clear about the waste wide range that exists between least and most hazardous residuals: Natural inorganic salts and sediments < Waste Heat < Organic wastes < Trace metals < Synthetic organic chemicals < Radioactive materials < Chemical and biological warfare agents. Obviously, environmental strategies must be commensurate with the substance of which disposal is required, as considering 'wide dispersal' (this is, diluting pollution through water discharge) suitable for harmless residual wastes.

To carry out this precise dilution method, hydraulic engineers have reached the solution with structures to produce a submerged effluent, called submarine outfalls, that emanates residual waste plumes. The analysis of buoyant jets or plumes depends not only on the jet parameters but also on the ambient conditions represented by the ambient density stratification and the

current profile. Only initial mixing of a discharge can be controlled by the engineer, based on design characteristics. Therefore, the dispersion already depends on the movement the seawater follows. This initial dilution by the diffuser is 10 times bigger than the subsequent mixing at the sea for a period of few hours (Fischer *et al.*, 1979).

2.3.1. 'Submarine Diffuser Model' methodology

The mixing phenomena methodology and its *formulae* (Brooks, 1973), that hydraulic engineers had in consideration to model the submarine diffusers, is explained in the following lines:

As the diffuser length sometimes can be up to 10 times its depth, it must be considered as a two dimensions problem, as it's shown in Figure 5.

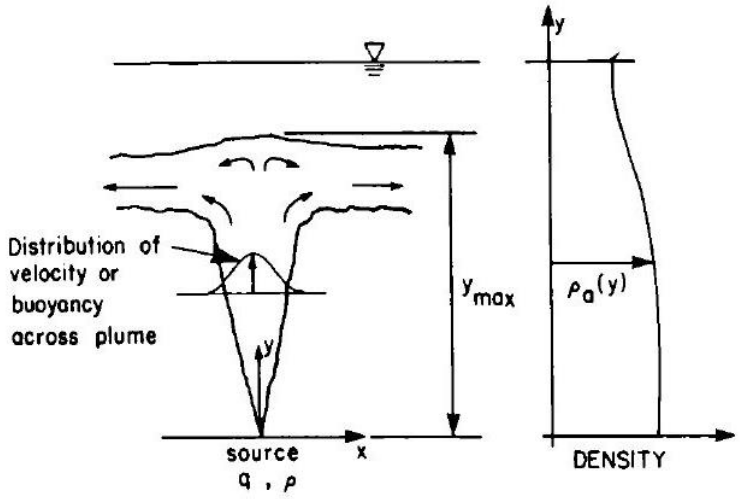

Figure 5. Schematic 2D-section drawing of a plume from a submerged diffuser (Fischer, 1979)

In general, diffusors are made of a series of aligned holes through which individual and circular jets emerge, but tend to merge and create a curtain of infinite groove jet. Knowing that all buoyant discharges tend to flow and follow a plume distribution, a very useful result is the following formula that estimates the dilution of the plume for a non-stratified and uniform ambient:

$$S = 0{,}38 * \frac{g'^{1/3} * d}{q^{2/3}} \quad (1)$$

$$\text{with} \quad g' = g * \frac{\rho' - \rho}{\rho} \quad (2)$$

S: centerline dilution [Ø]
g': modified gravitational acceleration [m/s^2]
d: vertical distance above the source [m]
q: initial discharge flow per unit length [m^2/s]

g: gravitational acceleration [m/s^2]
ρ': density of the ambient fluid [kg/m^3]
ρ: density of the discharged fluid [kg/m^3]

From these equations we can assume that dilution can be increased either by decreasing the initial discharge flow per unit length (this is, discharging less fluid or having a longer diffuser) or increasing the vertical distance above the source, which not always can be modified.

If the ambient fluid is not in a uniform density profile and stratification exists with a linear density profile, the previous formula has some changes. The new one is as follows:

$$S = 0{,}31 * \frac{g'^{1/3} * y_{max}}{q^{2/3}} \quad (3)$$

$$\text{with} \quad g' = g * \frac{\rho' - \rho}{\rho} \quad (4)$$

$$\text{with} \quad y_{max} = 2{,}84 * (g' * q)^{1/3} * \left\{\frac{-g}{\rho} * \frac{d\rho_a}{dy}\right\}^{-1/2} \quad (5)$$

y_{max}: maximum height of rise of the plume [m]
ρ': density of the ambient fluid at the level of the discharge [kg/m^3]
$\rho_a(y)$: ambient density as a function of depth [kg/m^3]

In this case, y_{max} can differ from the total depth d because of the existing difference in density in the ambient zone. Due to this, the plume fluid raises up to a level where densities of both discharged fluid and ambient fluid are even, staying stabilizes at that depth as its vertical movement is zero. Then, when it reaches y_{max}, it diffuses horizontally. These formulas do not take into account ocean currents and the probability of '*non-linear*' density stratification.

At this point, when the discharge loses vertical speed and stabilizes horizontally, currents start influencing it. Only currents parallel to the diffuser are considered, since this case is about coastal aquifers and in those areas the current is parallel to the coastline. On the other hand, it is assumed that there is no diffusion by current in the first section of the plume in which the discharge rises floating, just as it is assumed that the two-dimensional problem refers to an infinite diffuser and not a finite one as in reality, because the Diffusion at the lateral edges of the finite plume cannot be characterized by these formulas and the new problem would be too complex.

As density is a function of both temperature and salinity, stratification is usually magnified in summer months when the sun raises the temperature of the sea only in the most superficial layers, as well as in the rainy seasons when they reduce the salinity level of the surface layer.

The coefficients in these equations have not been confirmed by experiments but are based on assuming that the entrainment process is unaffected by the stratification, so these techniques are only appropriate to have approximate results (data accuracy may vary by ±20%) (Fischer *et al.*, 1979).

2.4. Method nº2: Estuaries – 'Boxes Model' methodology

As said before, estuaries are those places where continental waters join the ocean ones. A more classic definition for this term, frequently used in literature about this topic, was given by (Cameron and Pritchard, 1963), who defined estuaries as 'a semi-enclosed body of water which has a free connection to the open sea and within which seawater is measurably diluted with freshwater derived from land drainage'.

The mixing analysis by interaction between advection and diffusion flow is very complicated in estuaries. The best way to understand it is by differentiating the effect of the three main sources of mixing and analyzing it separately: wind, tides and river (Fischer *et al.*, 1979). First, the wind causes a movement towards its own direction in shallow waters, while in deeper waters, the average direction of the movement of water is in the opposite direction to the wind (generally, this occurs in shallower basins). This is because the net force produced by the wind is located in the centroid of the surface, while the centroid of the water body is in a deeper part, creating a torque that will induce rotational motion. Second, tidal currents are produced by the oscillation of the height of the water column due to astronomical tide (stars' attraction) and the meteorological tide (atmospheric pressure and winds).

Third, the process that affects long-term circulation in estuaries is mainly this freshwater supply from this land drainage. The differences in density between incoming freshwater and the ocean water imply a density gradient which creates currents, enhancing water movement from inland to offshore areas (Officer, 1983). Generally, less dense freshwater flows over the denser saltwater, even though in some specific estuary types the water mass movements can be different. Due to this continuous movement between layers of water, turbulence is generated in the interface causing a mixing effect partially reducing their density difference (Rattray and Hansen, 1962 and Officer, 1976).

The estuary circulation can be 'positive' or 'negative' (Pritchard, 1952): coastal lagoons are very similar to estuaries, but as they have no connections to freshwater, water evaporates and their salinities increase thus promoting the appearance of a density gradient, opposite to that of the estuaries with fresh water supply described previously (positive estuaries), that causes the circulation of seawater into the lagoon (negative estuaries).

A very common way to classify coastal estuaries or lagoons is to divide them into three types according to their vertical salinity profiles (Cameron and Pritchard, 1963):

- Salt-Wedge Estuary: This is a type of estuary where the contribution or flow of the river is huge and there are no significant tides or very small ones. A perfect example of a salt-wedge estuary could be the estuary of the Ebro river in Spain, discharging water to the Mediterranean Sea. As tides act in coastal areas as the principal mixing factor, its absence allows a strong stratification, thus vertical salinity profile changes are very acute. The river freshwater flows above seawater, and there is a very thin 'salinity transition zone' (halocline) where no mixing will occur, or they hardly mix. The halocline is very horizontal, and there is a lot of difference between the freshwater salinity and

the one form the sea. In the vertical velocity profile, the wedge moves very slowly, and vertical mixing coefficient 'Kz' is minimal. Therefore, a difference in salinity usually means also differences in density, creating strong density gradient and an acute pycnocline.

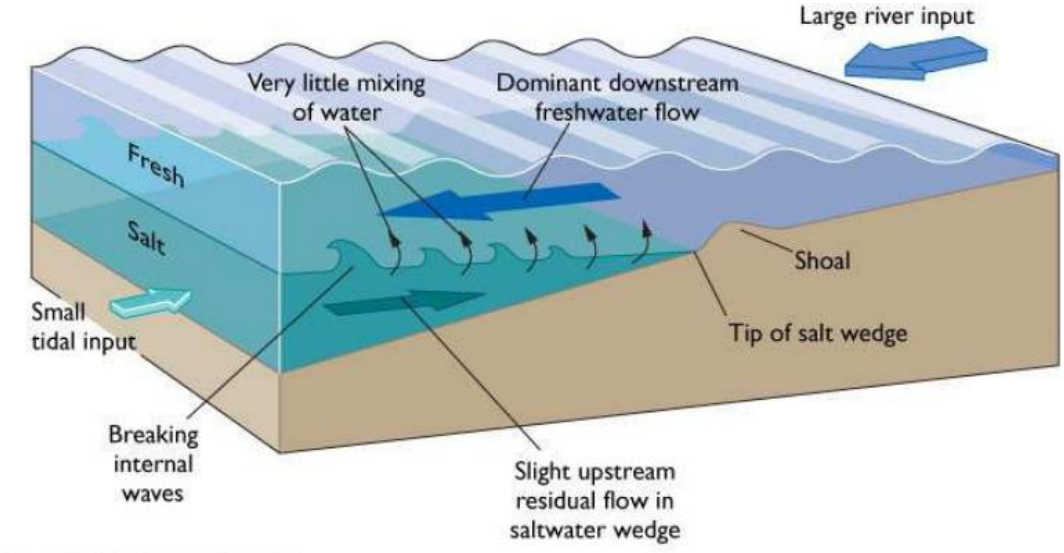

Figure 6. Salt-Wedge Estuary scheme (Pinet, 2013)

- Partially Mixed Estuary: This type of estuary occurs basically in zones where tides have a lot of mixing capacity (i.e. in Atlantic areas), and the tide itself is the mixing agent. Due to this powerful vertical mixing, the stratification is no longer as pronounced as in the salt-wedge estuary, and the halocline is more stretched and less horizontal. The intermediate zone has a lot of interaction between seawater and the river freshwater, being quite high the vertical mixing coefficient 'Kz'.

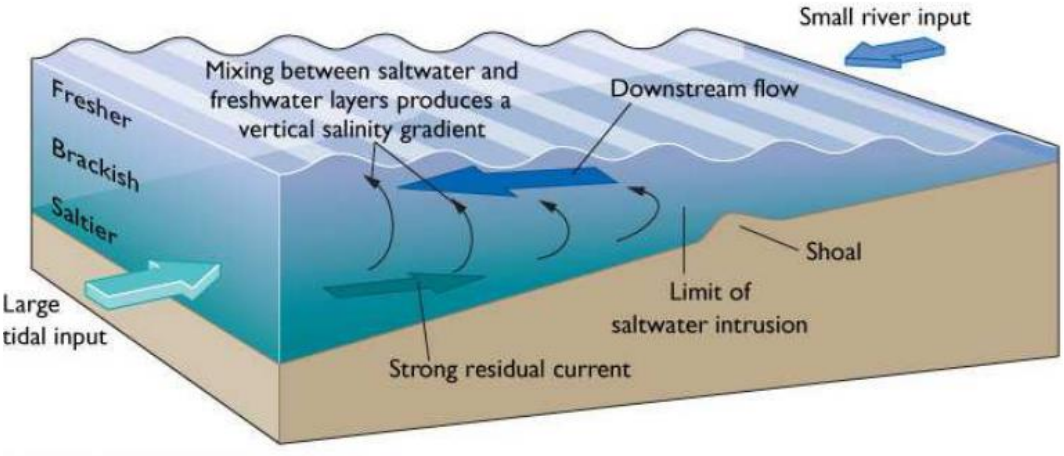

Figure 7. Partially Mixed Estuary scheme (Pinet, 2013)

- Well-Mixed Estuary: In this case, the estuary is also under significant tidal effect and its with is high enough (order of magnitude of several kilometers) that the 'Coriolis force' deflects trajectories of water masses to the right or left. The river freshwater flows out

towards the open sea, but it drifts to the right becoming in this case in a horizontally distributed estuary. The water masses are placed next to each other, while the river freshwater sticks to the right bank of the sea water and vice versa. This horizontal distribution creates a shear flow that causes the appearance of a lateral mixing, much stronger than the vertical one seen before. With this shear flow, mixing, and with ocean tides, the mixing is way bigger than in the other two conditions and, with it, the stratification disappears and transforms to a very homogeneous salinity profile. Although vertical mixing here is non-existent, the horizontal mixing 'Kh' is very high.

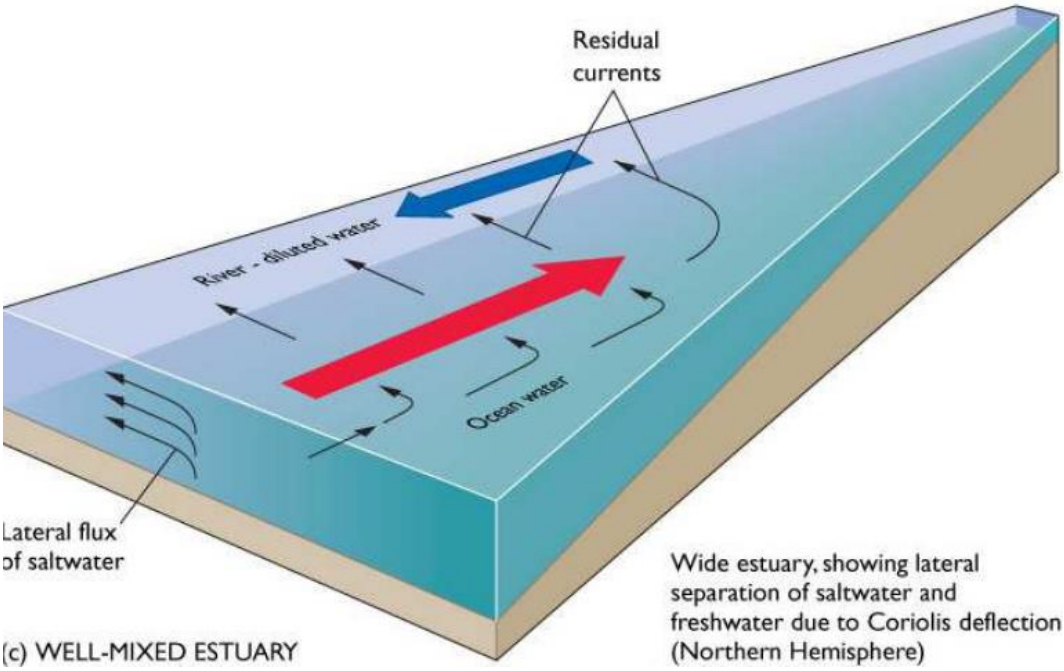

Figure 8. Well-Mixed Estuary scheme (Pinet, 2013)

From a hydrodynamic point of view an estuary can be characterized in many other ways as in (Hansen and Rattray 1966, Dalrymple *et al.* 1992 or Dyer 1997). Besides the three estuary types mentioned above, all range of variants and intermediate cases of partially mixed estuaries should also be considered (Cameron and Pritchard, 1965).

In Figure 9 these estuarine circulation patterns can be seen synthetized in a summary with their characteristics.

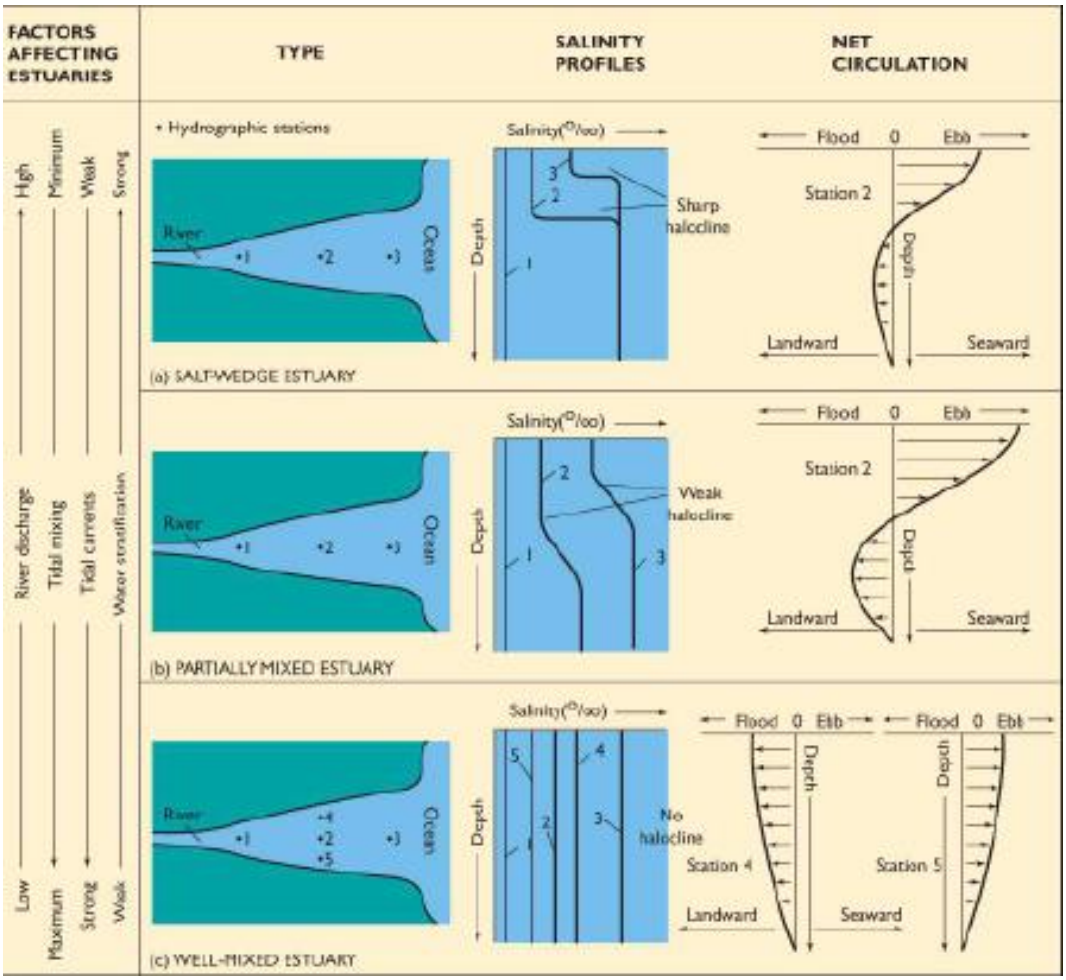

Figure 9. Summary of factors affecting estuaries (Pinet, 2013)

2.4.1. 'Boxes Model' methodology

A method to quantify inflows and outflows to and from the estuary system is the steady-state 'Box Model' used in several studies developed by (Munekage and Kimura 1985, Suzuki and Matsukawa 1987, Matsukawa and Sasaki 1990, Babenerd 1991, Norro and Frankignoulle 1996, Flindt and Kamp-Nielsen 1997, Justic et al. 1997, Hagy et al. 2000). This methodology takes into account salinity gradients that induce differences in densities, causing net flows of freshwater from the estuary to the ocean and vice versa with recirculated saltwater.

Considering the adequate divisions to the estuary and defining the corresponding existing flows between these division boxes, the 'Box Model' is useful to provide a solution to the convenient system of equations and thus be able to know the internal flows between the volumes of water of the studied space and the existing flows that enters and leaves it.

Only valid results will be given by the application of this methodology if a steady-state system is considered. That would not be the case if, between two established time moments, the studied water body changes in water volume or if its salt content does not remain constant (this is,

changes over time). Thus formulas 6 and 7 are the needed hypothesis to consider an estuary as a valid study area.

$$\frac{\delta V}{\delta t} = 0 \qquad (6)$$

$$\frac{\delta S}{\delta t} = 0 \qquad (7)$$

As an example, the following figure will show the scheme adopted for the box model that (de Pedro, 2007) considers in his study of three discharges of freshwater through rice crop canals in the Ebro Delta, and the corresponding system of equations to fulfill the conservative conditions (examples for boxes 2 and 5):

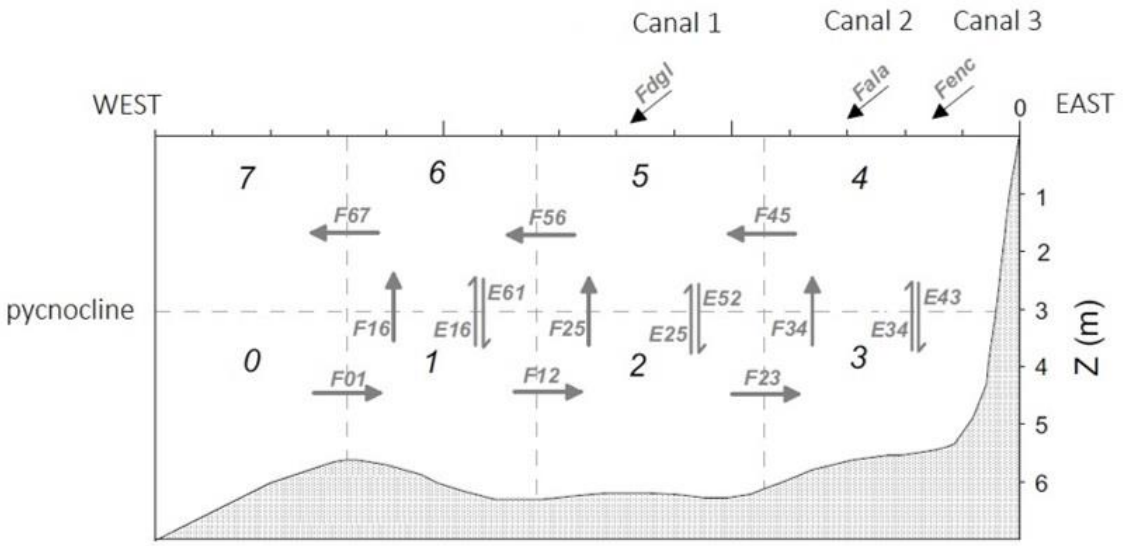

Salinity Balance:

(2) $F_{12} * S_1 + E_{52} * S_5 = F_{25} * S_2 + E_{25} * S_2 + F_{23} * S_2$

(5) $F_{dgl} * S_{dgl} + F_{45} * S_4 + F_{25} * S_2 + E_{25} * S_2 = F_{56} * S_5 + E_{52} * S_5$

Volume Balance:

(2) $F_{12} = F_{25} + F_{23}$

(5) $F_{dgl} + F_{45} + F_{25} = F_{56}$

Figure 10. Box model scheme example, modified from (de Pedro, 2007) and some examples of its equation systems

Later, in point 4. ‘Materials and Methodology’, the decisions taken in this specific study, the definitions of variables and other considerations to take into account for the methodology of the ‘Boxes Model’ will be specified with more details (specifically in point 4.3. ‘Adaptation for Proposal nº2’).

3. AIM OF THE PROJECT

As commented before, the critical situation that the world is suffering, where climate change and land over-exploitation that produce an increase of the sea level and subsequent intrusion of saltwater in coastal aquifers.

Several scientific studies have been carried out in the field of SWI or SGD, such as (Huyakorn et al., 1987), (Pool and Carrera, 2010) or (Wener et al., 2013), but even nowadays the process for SGD identification, qualification and quantification is quite far from being a safe bet. The principal reason that the estimation of groundwater has not reached the precision base that is typically achieved of other oceanic inputs is that the direct discharge of groundwater into the coastal zone is difficult and complex to measure. In order to develop the scientific and technical knowledge that will enable these measurements to be addressed with a higher degree of confidence, a group of scientists ran a series of intercomparison experiments to evaluate SGD assessment techniques (Burnet et al., 2008). (Garcia-Solsona et al., 2010) explain how their SGD considerations need to consider a possible fluctuation of around a 10 or 20% of the obtained result.

In order to better understand the processes that control the advance and retreat of the interface between freshwater and saltwater in coastal aquifers, studying the hydrodynamics behind Submarine Groundwater Surges, the general objective of this study is to compare the SGD process with a submarine outfall discharge and/or a submarine estuary spill in order to calculate the FSGD fluxes in an alternative way.

And in order to arrive to this general objective, the partial objectives of this work are summarized in the following points:

- To study the distributions of temperature, salinity and other marine and meteorological properties of different scenarios with surges of different characteristics.
- To approach and adapt two different methodologies for FSGD flux calculation to use in the studied upwellings.
- To calculate the upwelling fluxes and other fluxes both convective and diffusive (in the case of the box model methodology).
- To analyze the obtained results and to evaluate the proposed methods.

4. MATERIALS AND METHOD

4.1. Data collection

4.1.1. First study area (Castellón)

This first study area is located on the west coast of the Iberian Peninsula, more specifically in Castellón, a province of the Valencian Autonomic Community. "Torre Badum" is located about 55 km north of the city of Castellón and 5,5 km from the coastal city of Peñíscola, as shown in Figure 11. It is an open coastal zone, and the length of the upwelling extends between 50 m and a maximum of a couple of hundred meters, on the in the coastline adjacent to “Torre Badum”, discharging freshwater to the Mediterranean Sea.

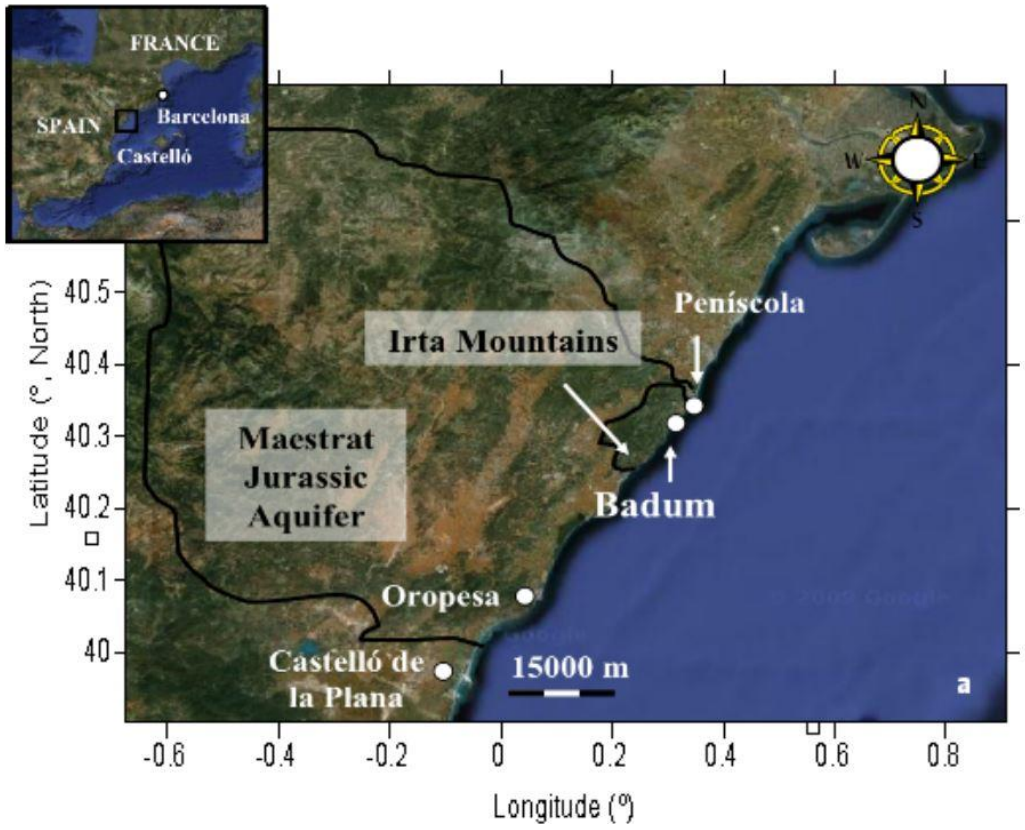

Figure 11. Torre Badum situation on a satellite map of the Valencia coastline in Castellón (García-Solsona, 2010)

The onshore coastal part of the study area has a well-developed karstic structure.

This kind of geological structures tend to be quite common in many coastal areas, especially on the coasts surrounding the Mediterranean Sea, where they represent up to 60% of the coastline (UNESCO, 2004). These are characterized by their high degree of cracking of the rock that composes them, produced by a natural geological process, which leads to highly permeable

aquifers that allow the percolation of water flows due to their breaks resulting in freshwater or saltwater outflows into the sea.

The littoral aquifer, named 'Aquifer of *El Maestrat*', is formed bay this karstic layer product of long sedimentation processes from the Jurassic era, which sits at great depths inland and extends towards coastal area until it outcrops (Mejías *et al.*, 2008). Some studies, as the one done by (Ballesteros, 1989), show how the geological formation of the study aquifer maintains ideal conditions for the filtration and flux of groundwater. Among the data that these studies give as a reference is the transitivity that varies between 1.000 and 15.000 m^2/d.

Figure 12. Karstic geological soil in Torre Badum (diariodekayak.es)

In this area, the annual precipitation usually ranges between 400 and 650 mm. This data oscillates according to seasonal phases of the typical Mediterranean regions, which can be wet and dry. Like many other karst areas, precipitation has no effect on the amount of surface runoff, except in the case of torrential rains, since as it is a terrain with a lot of gaps and fissures (Figure 12), the precipitation almost completely penetrates the ground. The fact that little surface runoff is generated in the study zone, implies the non-existence of river freshwater discharges to the sea, since it mostly occurs at submarine levels through the aquifers. Also due to the absence of rivers and their transport of fine sediments, the immediate seabed of the coastal aquifer is made up of coarse-grained sand. As for the wind, the strong breeze causes the coastal waters to mix with the open sea on short time scales (García-Solsona *et al.*, 2010).

The deep aquifer of 'El Maestrat' is the main and only hydrogeological agent that contributes to the groundwater coastal discharge to the maritime study area. This discharge is carried out through three coastal springs: from smaller to larger, the first is located on Peñíscola's beach,

the second is identified in Alcocebre another city located further south than our study area and the third, the one that discharges the largest volume of water, is the one in our study in Torre Badum. Thermal infrared airborne images (TIR) allowed identifying Torre Badum as the main area where the aquifer discharges freshwater through an SGD, as shown in (Figure 13).

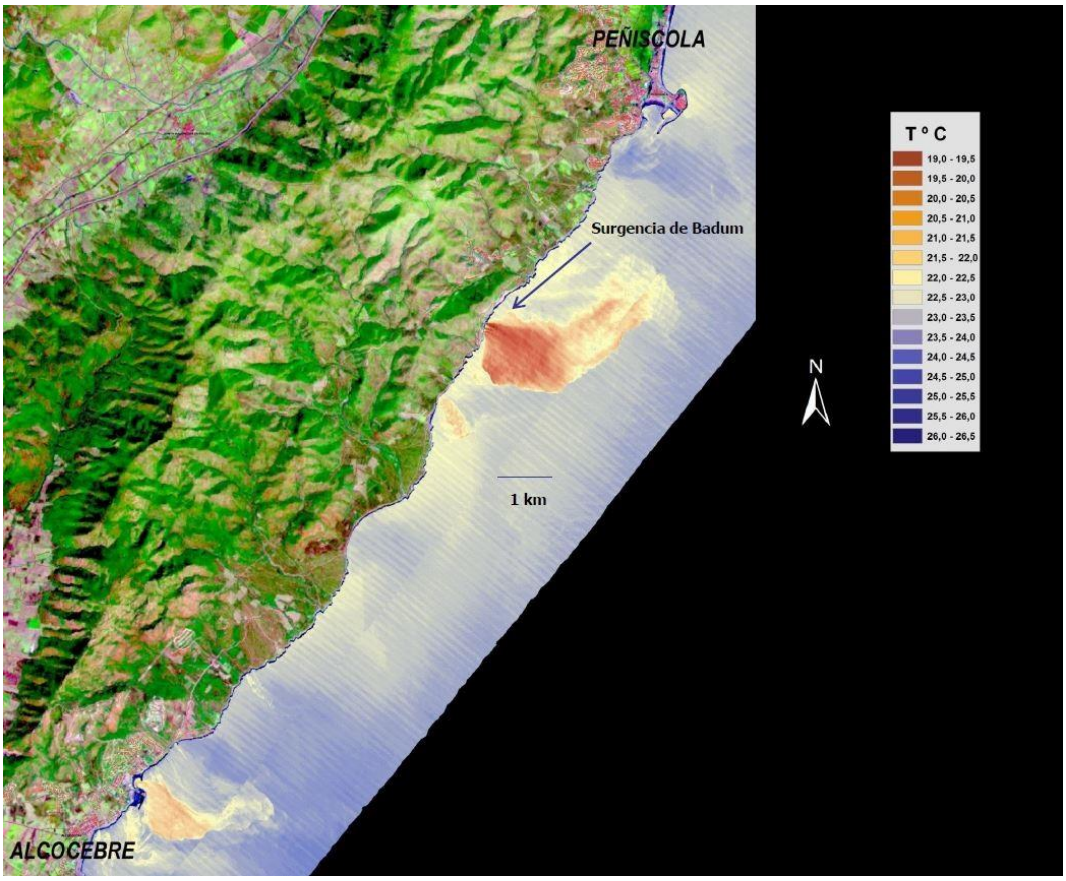

Figure 13. Identification and mapping of coastal SGDs in the karst aquifer of 'El Maestrazgo' (Castellón) using remote sensing techniques from airborne Thermal Infrared (TIR) (García-Solsona, 2010)

In order to analyze the areas where the Jurassic aquifer of 'El Maestrazgo' affects the ecosystem by SGD, several techniques have been applied to identify the upwelling and to quantify its flux, among which are the thermal infrared images (TIR) collected by airborne vehicles or satellites, the collection of in-situ data such as salinity or temperature, and the activity of ^{222}Rn. This last technique has been widely used in many oceanographic research campaigns, proving to be suitable for the case study of coastal karst aquifers (Mejías *et al.*, 2012).

Hydrological models were used to provide the first estimates of the SGD flow that the coastal springs of the 'Irta' mountain range discharged into the sea. Together with subsequent studies and a mathematical model specifically designed for the coastal aquifer sector, a fresh water and recirculated saltwater discharge of 64 x 10^6 m^3/year was estimated, that is, about 175 x 10^3 m3/day (Ballesteros, 1989).

4.1.1.1. Ocean and meteorological data

4.1.1.1.1. Castellón, October 2006

On one hand, to obtain the ocean data, a sampling in the coastal area of Torre Badum that was carried out in October 2006 is used (Figure 14). In this data campaign, samples of seawater were obtained for different purposes, among which are Radio isotopes (^{223}Ra or ^{224}Ra isotopes are usually the most used for this type of studies), dissolved inorganic nutrients (NO_2^-, NO_3^-, NH_4^+, PO_4^{3-}, and SIO_4^{2-}) and the main dissolved elements that can normally be found in these waters (Ba, Br, Ca, Cl, K, S and Sr). In brief, 50 liters were taken for analysis, all of them at an average depth of 20 cm more or less. To obtain information the submarine groundwater discharge source, it has been used data from the same campaign too, extracting water samples directly from the spring with a submersible pump. From those samples, same water properties as in the samples taken of seawater were analyzed (García-Solsona *et al.*, 2010).

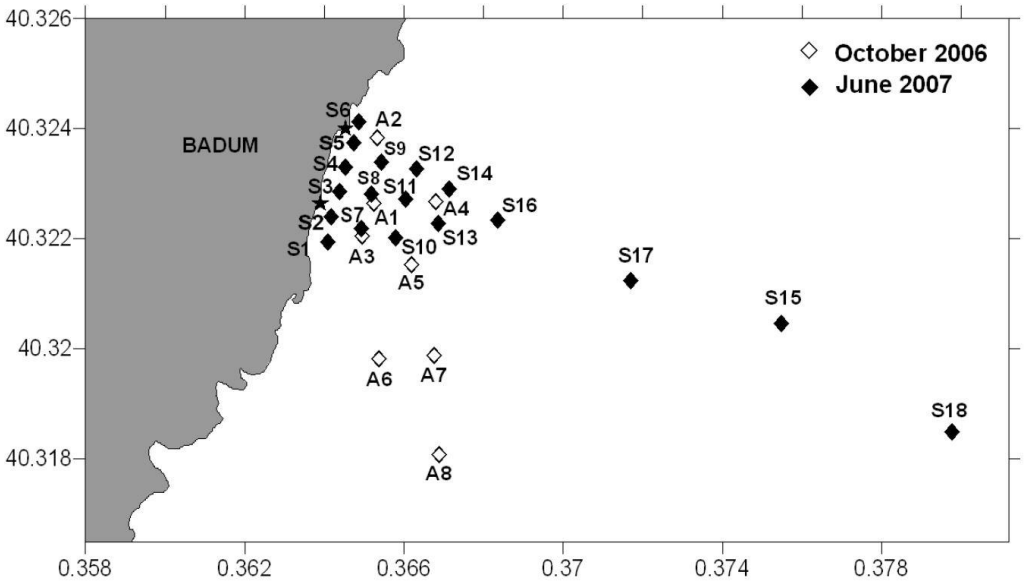

Figure 14. Water stations' location for seawater data. Two different campaigns can be distinguished, one form October 2006 and another from June 2007. (García-Solsona, 2010)

Both the water to analyze the dissolved inorganic nutrients and the main elements, were collected in polypropylene bottles to then be instantly frozen and kept that way until their analysis in the laboratory. The dissolved inorganic nutrients were analyzed by an 'auto-analyzer' and the main elements by an X-ray fluorescence process. As for the temperature and salinity of the SGD source and plume, a laboratory calibrated handheld multi-parameter probe was used to record them in the study zone. Connected to a GPS, the data was recorded at the same time geographic position was monitored.

The following (table 1) shows the data obtained from this campaign. On it, the concept 'DIN' is used to refer to the sum of NO− 3, NO− 2 and NH + 4. For the same reason, 'DIP' is defined as the sum of PO3− 4 and 'DSi' like that of SiO4.

Station number	T (°C)	Sal	Ra activity (dpm 100L^{-1}) ^{223}Ra	^{224}Ra	^{226}Ra	^{228}Ra	Nutrient concentration (μM) DIN	DIP	DSi
October sampling (24/10/2006)									
Surface coastal waters									
A1	20.4	27.1	10.1±1.1	111±7	130±2	91±2	23.8	0.13	25.3
A2	20.2	25.3	10.2±1.7	132±7	142±2	100±2	37.6	0.17	32.7
A3	20.0	23.5	10.5±0.8	156±7	142±6	114±3	34.5	0.18	35.7
A4	21.1	30.2	7.6±0.9	90±6	104±5	69±2	20.8	0.11	18.6
A5	20.8	28.6	8.1±1.4	105±5	121±5	87±2	24.9	0.13	19.2
A6	21.3	32.0	4.6±0.5	76±3	87±4	57±2	26.4	0.11	14.2
A8	21.3	33.0	4.4±0.4	73±3	71±3	50±2	28.2	0.08	13.1
Average coastal waters									
	20.7	28.5	8±2	106±30	114±27	81±23	28.0	0.13	22.7
Springs									
A-SP1	19.4	13.7	13.2±1.2	227±11	254±2	185±4	28.5	0.36	66.2
A-SP2	19.1	8.7	21.5±1.6	253±12	261.5±1.7	212±4			
Seawater: out of the fresher plume water									
A7	21.8	38.2	2.2±0.4	19.0±1.6	32±2	8.7±1.7	2.3	0.08	1.46

Table 1. Temperature (T), salinity (S), Radium activity and nutrient concentrations for every single station of the October 2006 campaign. (García-Solsona, 2010)

García-Solsona, (2010) gives as result of the 24th October 2006 campaign study an SGD flux in Torre Badum of 71.500 ± 11.200 m^3/day. Knowing the source salinity (average S_{SGD} = 11,2), FSGD flux can be obtained and is estimated to be 50.500 m^3/day, this is 18,44 Mm^3/year.

On the other hand, to obtain the historical meteorological data, a series of public and open data banks have been analyzed. Due to the quantity and quality of the data provided in each of them, it was finally decided to use the website (climate-data.org) as a data source for our study. The data obtained from this website that is necessary to carry out the calculation process for the used methodologies will be explained below:

Meteorological Data	
Average atmosphere temperature on 24th October 2006, from 00:00 a.m. to 11:59 p.m. of the data campaign day	18 ºC
Daily average atmosphere temperature range on the data campaign day	9 ºC
Difference between the mean temperature of the hottest month (August) minus the mean temperature of the coldest month (January)	15 ºC
Hours of solar radiation on the data campaign day	10,78 hours (10 h and 47 min)

Precipitation on the data campaign day	1,6 mm/day (49,6 l/(m^2*month))
Cloudiness percentage on the data campaign day	50 %

Table 2. Meteorological data from Torre Badum needed for the methodology, 24th October 2006 (source: climate-data.org)

In addition, other data needed to perform calculations are listed below:

- The area covered by the SGD plume: approximately 1,15 km^2
- Latitude of the source point at Torre Badum: 40 º 19' 26,73'' N
- Altitude of the source point at Torre Badum: 0m (obviously, at sea level)
- Length of the plume orthogonal to the coastline: 1500 meters
- Width of the SGD source along the coastline: approximately 75 meters
- Width of the plume: approximately 0,5 meters

Both the plume's area and the source width are obtained from the infrared imagery such as Figure 13 (not exact data). Instead, for the width of the plume, the data was determined by the value that (Garcia-Solsona, 2010) gives us.

4.1.1.1.2. Castellón, June 2007

On the one hand, it seems reasonable to take the same scenario with other data as a first candidate to contrast some results. So, having another data campaign carried out also in the 'Irta' mountain range coastline, this time in the month of June 2007, makes it easier for some data collection reasons, and at the same time the dates make them different enough to carry out a data contrast.

This time, as in the October campaign, seawater samples were taken to the laboratory to analyze Radium activity (223Ra and 224Ra isotopes), dissolved inorganic nutrients (NO_2^-, NO_3^-, NH_4^+, PO_4^{3-}, and SIO_4^{2-}) and the main dissolved elements that can normally be found in these waters (Ba, Br, Ca, Cl, K, S and Sr). Salinity and temperature were measured in-situ as explained before, in the June stations' locations shown in (Figure 14).

(Table 3) presents the data obtained from this subsequent 'summer campaign':

Station number	T (°C)	Sal	Ra activity (dpm 100L^{-1}) ^{223}Ra	^{224}Ra	^{226}Ra	^{228}Ra	Nutrient concentration (μM) DIN	DIP	DSi
June Sampling (4-6/06/2007)									
Surface coastal waters									
S1	20.1	28.3	4.8±0.3	54±2	64.9±1.4	42.8±1.7	24.2	0.29	20.8
S2	21.2	32.2	3.8±0.2	53.3±1.8	52±2	34.4±1.7	19.6	0.39	13.5
S3	20.1	18.9	6.2±0.7	98±3	119±5	87±3	38.1	0.34	21.1
S4	21.7	28.0	4.7±1.1	63±9	73±3	56.2±1.9	20.8	0.44	16.8
S5	21.8	33.8	2.8±0.2	32±2	37.8±1.8	25.6±1.1	13.7	0.35	10.6
S6b	19.0	16.8	5.1±0.6	124±4	137±6	104±3	56.3	0.39	36.6
S7	19.8	26.9	4.1±1.0	74±10	63.8±1.5	46.3±1.7	34.2	0.38	30.7
S8	19.1	21.7	6.0±0.4	95±3	113.2±1.8	79.6±1.7	50.9	0.4	36.8
S9	19.5	16.6	8.8±0.5	108±4	118±6	96±3	69.6	0.44	46.6
S10	19.2	22.3	6.1±0.7	80±3	109±5	79±2	46.3	0.36	32.9
S11	19.1	21.0	7.2±1.8	92±13	77.7±1.7	74±3	50.8	0.39	35.7
S12	19.6	27.7	4.4±0.4	57±2	55±3	58±3	32.1	0.34	26.1
S13	19.0	19.3	7.0±0.4	117±3	119±5	91±2	44.1	0.37	31.8
S14	18.8	14.5	8.7±1.0	127±4	154±7	105±3	59.5	0.43	42.9
S15	20.9	37.0	1.6±0.4	23±7	20.5±1.3	15.0±1.5	7.3	0.23	3.2
S17	21.4	27.0	4.2±0.3	67±2	66.0±1.2	49.7±1.2	27.3	0.27	22.9
S18	20.2	23.3	4.9±0.3	96±3	75.5±1.8	66±2	38.7	0.32	28.3
Average coastal waters									
	20.0	24.4	6±2	86±40	85±40	63±29	37.3	0.36	26.9
Coastal waters at 50 cm depth									
S8 –50	36.3	20.4	2.5±0.3	32.3±1.3	22.1±1.6	15.0±1.4	10.4	0.27	8.1
S11 –50	36.0	20.6	2.3±0.2	29.9±1.0	25.0±0.7	16.1±1.0	9.0	0.25	9.6
S13 –50	36.0	21.1	2.2±0.2	31.0±1.1	23.1±0.7	14.8±1.0	9.6	0.26	5.5
Springs									
S-SP1	18.4	5.5	9.6±1.3	158±8	189±9	140±4	114.1	0.53	57.1
S-SP2	18.2	5.5	3.1±1.0	175±25	157±3	139±5	74.7	0.38	36.2
Seawater: out of the fresher plume water									
S16	21.6	37.8	0.9±0.2	6.9±0.6	16.1±0.6	7.6±0.7	4.02	0.23	1.1

Table 3. Temperature (T), salinity (S), Radium activity and nutrient concentrations for every single station of the June 2007 campaign. (García-Solsona, 2010)

García-Solsona, (2010) gives as result of the June 2006 campaign study an SGD flux in Torre Badum of 187.000 ± 23.000 m^3/day. Knowing the source salinity (average S_{SGD} = 5,5), FSGD flux can be obtained and is estimated to be 159.400 m^3/day, this is 51,8 Mm^3/year.

At first, it can be seen how both plume water and source water are colder and also fresher in the month of June than in the month of October (temperature almost 1 ºC lower and more than 4 g/l less in salt content). Another detail to take into account from this table is summer water having higher nutrient rates and lower Radium activity.

Meteorological data also varies from October to June. Required data, taken from the same website as previously named, is enlisted right below:

Meteorological Data

Average atmosphere temperature on 4th-6th June 2007, from 00:00 a.m. to 11:59 p.m. of the data campaign day	22 ºC
Daily average atmosphere temperature range on the data campaign day	8,9 ºC
Difference between the mean temperature of the hottest month (August) minus the mean temperature of the coldest month (January)	15 ºC
Hours of solar radiation on the data campaign day	14,93 hours (14 h and 56 min)
Precipitation on the data campaign day	1,13 mm/day (35 l/(m^2*month))
Cloudiness percentage on the data campaign day	42,6 %

Table 4. Meteorological data from Torre Badum needed for the methodology, 4th-6th June 2007 (source: climate-data.org)

As in the previous campaign, geographic and geometric data needed to perform calculations are listed below:

- The area covered by the SGD plume: 1,85 km^2
- Latitude of the source point at Torre Badum: 40 º 19’ 26,73’’ N (does not change)
- Altitude of the source point at Torre Badum: 0m (obviously, at sea level)
- Length of the plume orthogonal to the coastline: 1.950 meters
- Width of the SGD source along the coastline: approximately 145 meters
- Width of the plume: approximately 0,5 meters

4.1.2. Second study area: Hawaii (August 2006)

In order to better understand and validate the application of the two proposed methodologies in the Submarine Groundwater Discharge in Torre Badum, by applying the same analysis process in other key emplacements where the presence of submarine upwellings make the comparison process possible.

For this reason, a second applicable data location comparable to the first one has been obtained because it is the same SGD but with slightly modified data due to differences in year seasons, the following step is to further test the methodology. Similar SGD conditions may lead one to think that precisely this type of scenario is suitable for the model, so marine areas that are

sufficiently different has been sought to consolidate the well-functioning of the method or, if this is not the case, to reboot the hypothesis of its potential and see which and where the weaknesses may be.

It has been decided to use (Peterson *et al.*, 2009) study to take a further step in the analysis. Their article talks about the presence of point source groundwater discharges to the ocean from the coast of the Hawaiian island called 'Big Island'. In it, they seek to locate and quantify the numerous upwellings present on the west coast of the island. In this case, it has been considered convenient to use its database to test our model and, among the different options, it has been decided to take the data from the upwelling of 'Kahauloa Bay' (Figure 15).

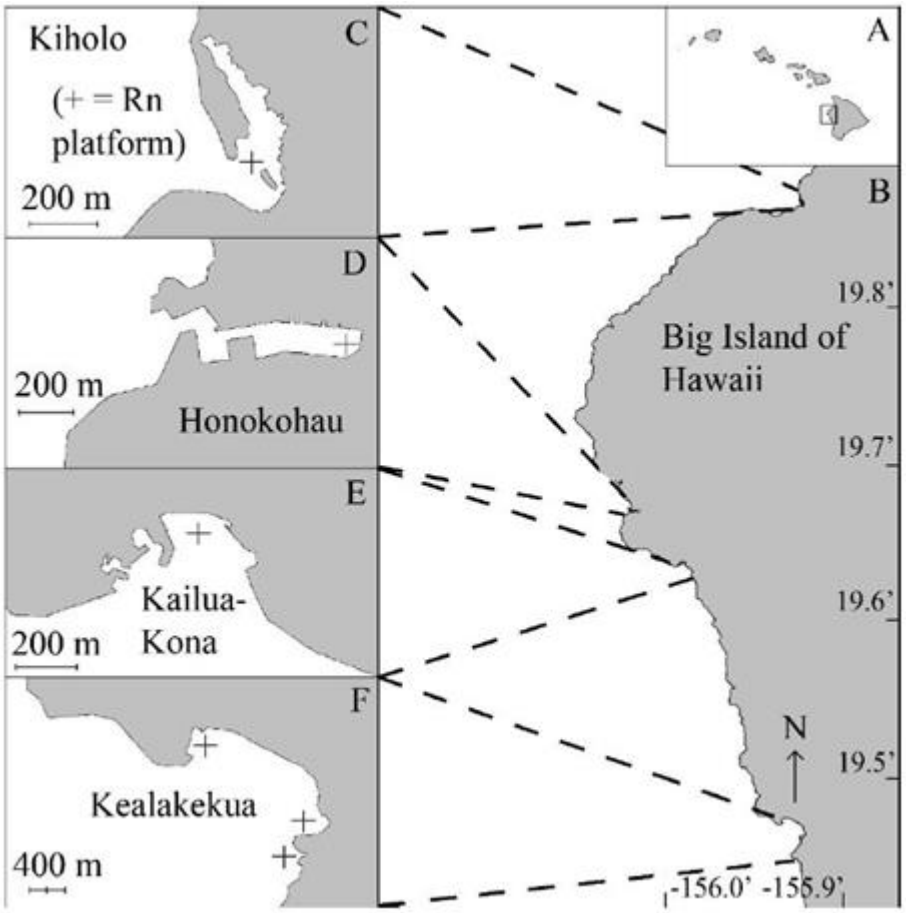

Figure 15. Map of the island chain (A) of Hawaii, with the west coast (B) of the Big Island of Hawaii. Each plus symbol represents the position of the radon shelf in the groundwater columns associated with study zones. Our selected area is (F) Kahauloa Bay (southeast) in Kealakekua Bay (Peterson *et al.*, 2009).

The bay where the chosen upwelling is located (Kealakekua Bay) and the adjoining bays in the Kaloko-Honokohau National Historical Park area lie on the arid and desert leeward coast of the Big Island, where river inlets are practically non-existent. Submarine groundwater flowing out of the coastal zone thus controls practically the entire freshwater supply to this vast region. These more than 30 point-sourced nutrient-rich massive plumes of cool groundwater discharge into the coastal zone, are the sole source of new nutrient delivery to coastal waters in this oligotrophic setting. Water column profiling and nutrient sampling show that the plumes are

cold, buoyant, nutrient-rich brackish mixtures of groundwater and seawater (Johnson *et al.*, 2008).

In the study zone of Kahauloa Bay, the annual precipitation usually ranges between 330 and 630 mm. In the middle of the Pacific Ocean, this location has significant tides and a coastline not straight, with many bays along this side of the island that allows the plume to mix but at the same time also creates a semi-enclosed water body in the bay. These characteristics are completely opposite to the coast of Torre Badum, which is completely exposed to the ocean and does not experience tidal processes.

The majority of the data needed to proceed with the calculations has been collected form the following tables of the Peterson *et al.*, (2009) study:

Reference no.	Well name	Description	Time-series site proximity	Used for groundwater end member?	Latitude	Longitude	Depth (m)
1	Kiholo Lagoon	Surface water sample	Kiholo		N19°51.633′	W155°55.334′	n/a
2	Fishpond	Brackish pond	Kiholo		N19°51.318′	W155°55.185′	n/a
3	Lava tube	Freshwater in lava tube	Kiholo		N19°51.242′	W155°55.386′	3.0
4	Energy lab—well 6	Natural Energy Laboratory	Honokohau		N19°43.600′	W156°03.569′	n/a
5	Energy lab—well 2	Natural Energy Laboratory	Honokohau		N19°42.754′	W156°02.906′	4.8
6	Hualalai well	Upland well	Honokohau		N19°42.250′	W155°58.438′	485.6
7	KNP-1	Kalako National Historical Park well 4161-01	Honokohau		N19°1.233′	W156°01.750′	7.2
8	KNP-2	Kalako National Historical Park well 4161-02	Honokohau		N19°41.155′	W156°01.409′	17.8
9	Honokohau well	Upland well	Honokohau		N19°40.940′	W155°57.865′	557.4
10	KNP-3	Kalako National Historical Park well 4161-03	Honokohau		N19°40.705′	W156°01.330′	12.0
11	HW-14	Honokohau Harbor expansion well	Honokohau	Honokohau	N19°40.120′	W156°01.083′	n/a
12	HW-15	Honokohau Harbor expansion well	Honokohau	Honokohau	N19°40.113′	W156°01.155′	9.2
13	HW-16	Honokohau Harbor expansion well	Honokohau	Honokohau	N19°40.083′	W156°01.211′	15.7
14	HW-17	Honokohau Harbor expansion well	Honokohau	Honokohau	N19°40.076′	W156°01.265′	16.4
15	HW-6	Honokohau Harbor expansion well	Honokohau	Honokohau	N19°39.976′	W156°01.419′	13.1
16	HW-9	Honokohau Harbor expansion well	Honokohau	Honokohau	N19°39.878′	W156°01.491′	18.0
17	Kahalo well A	Upland production well	Kailua-Kona		N19°34.978′	W155°56.988′	283.8
18	Kahalo well C	Upland production well	Kailua-Kona		N19°34.962′	W155°56.971′	288.7
19	Kahalo well B	Upland production well	Kailua-Kona		N19°34.904′	W155°56.983′	300.2
20	Kahalo well D	Upland production well	Kailua-Kona		N19°34.884′	W155°56.954′	295.3
21	Keauhou bath	Ancient Hawaiian bath	—		N19°33.666′	W155°57.703′	1.5
22	Halekii well	Upland production well	—		N19°31.087′	W155°54.974′	105.0
23	Queen's bath	Ancient Hawaiian bath	Queen's Bath/ Kahauloa	Queen's Bath/ Kahauloa	N19°28.907′	W155°55.997′	0.3
24	Kelly's well	Ancient Hawaiian well	Manini/ Kahauloa	Kahauloa	N19°28.258′	W155°55.238′	0.5
25	Manini bath	Ancient Hawaiian bath	Manini/ Kahauloa	Manini/ Kahauloa	N19°28.249′	W155°55.243′	0.3
26	Vergi's well	Ancient Hawaiian well	Kahauloa	Kahauloa	N19°28.180′	W155°55.261′	1.0
27	Keei well D	Upland production well	Kahauloa		N19°27.725′	W155°52.820′	353.3
28	City of Refuge	Brackish pond	Kahauloa	Kahauloa	N19°27.486′	W155°55.469′	1.0

Table 5. Reference data for every SGD location in the Hawaiian west coastline (Peterson et al., 2009)

From Table 5, reference numbers of the selected SGD are obtained, as well as geographic coordinates and other general data. Instead, in Table 6, a more precise maritime information is enlisted, among which temperature (T) and salinity (S) stand out. These properties belong to the

SGD source waters. To obtain data out of the upwelling source waters, Figure 16 and Figure 17 show Salinity and Temperature variability trough time and based on distance to the SGD source:

Reference no.	Date sampled	Salinity	Temperature (°C)	^{222}Rn (Bq m^{-3})	^{223}Ra (Bq m^{-3})	^{224}Ra (Bq m^{-3})	^{226}Ra (Bq m^{-3})	^{228}Ra (Bq m^{-3})
1	20 May 07	9.5	23.0	162±15	n/a	n/a	n/a	n/a
2	20 May 07	2.7	25.3	707±37	n/a	n/a	n/a	n/a
3	17 May 07	2.1	22.7	356±29	0.12±0.05	2.06±0.17	n/a	n/a
4	16 Feb 06	28.8	23.6	604±40	1.08±0.21	13.40±0.73	0.37±1.2	4.8±5.2
5	16 Feb 06	11.3	21.8	424±33	0.42±0.05	7.22±0.35	0.65±0.43	6.3±1.7
6	15 Feb 06	0.1	21.1	5730±120	BD	0.06±0.03	BD	BD
7	17 Aug 05	6.8	22.4	n/a	BD	2.76±0.36	n/a	n/a
	14 Feb 06	7.3	20.9	192±18	0.08±0.03	1.48±0.11	0.80±0.45	1.7±1.6
8	17 Aug 05	5.2	21.7	n/a	0.60±0.12	6.46±0.55	n/a	n/a
	14 Feb 06	5.8	23.8	611±56	0.14±0.08	2.65±0.39	1.3±1.7	0.2±6.3
9	15 Feb 06	0.1	21.8	1540±78	BD	0.22±0.08	BD	BD
10	17 Aug 05	11.5	22.5	n/a	0.19±0.11	1.27±0.23	n/a	n/a
	14 Feb 06	11.8	21.5	242±22	0.35±0.08	2.43±0.18	1.02±0.04	2.3±1.3
11	17 May 07	7.1	20.7	500±28	0.17±0.06	1.20±0.16	n/a	n/a
12	16 May 07	8.2	20.9	274±20	0.19±0.05	1.80±0.18	n/a	n/a
13	16 May 07	15.3	20.5	456±26	0.67±0.12	4.48±0.34	n/a	n/a
14	17 May 07	17.9	20.2	431±23	0.76±0.12	5.17±0.27	n/a	n/a
15	16 May 07	19.0	20.7	371±23	0.79±0.13	9.98±0.62	n/a	n/a
16	16 May 07	23.8	20.3	520±28	0.18±0.07	7.67±0.47	n/a	n/a
17	13 Feb 06	0.4	21.0	1450±48	BD	0.13±0.02	0.18±0.14	0.36±0.55
18	13 Feb 06	0.2	21.4	1140±50	BD	0.04±0.02	BD	1.06±0.93
19	13 Feb 06	0.5	21.0	1415±75	BD	0.26±0.06	0.19±0.49	1.9±1.7
20	13 Feb 06	0.4	21.0	1150±60	BD	BD	0.21±0.18	BD
21	09 Aug 06	4.9	22.0	321±18	0.02±0.01	0.28±0.03	BD	0.01±0.55
22	13 Feb 06	0.1	21.8	879±43	BD	BD	BD	BD
23	10 Aug 06	6.7	21.5	49±10	n/a	n/a	n/a	n/a
24	07 Aug 06	7.1	21.1	120±16	0.03±0.01	0.23±0.04	BD	0.39±0.74
25	06 Aug 06	5.1	22.2	86±14	0.06±0.01	0.73±0.09	BD	BD
	19 May 07	6.5	20.4	131±14	n/a	n/a	n/a	n/a
	19 May 07*	6.5	20.4	106±20	n/a	n/a	n/a	n/a
26	07 Aug 06	5.7	20.6	83±14	0.03±0.1	BD	BD	BD
27	13 Feb 06	0.1	19.8	340±26	BD	0.12±0.04	0.08±0.33	BD
	15 Feb 06	0.1	19.6	375±32	n/a	n/a	n/a	n/a
28	11 Aug 06	8.1	23.4	78±9	n/a	n/a	n/a	n/a

* Denotes a time-series record average of this well over 24 h.

Table 6. Temperature (T), salinity (S), Radium and Radon activity for every SGD location in the Hawaiian west coast (Peterson et al., 2009)

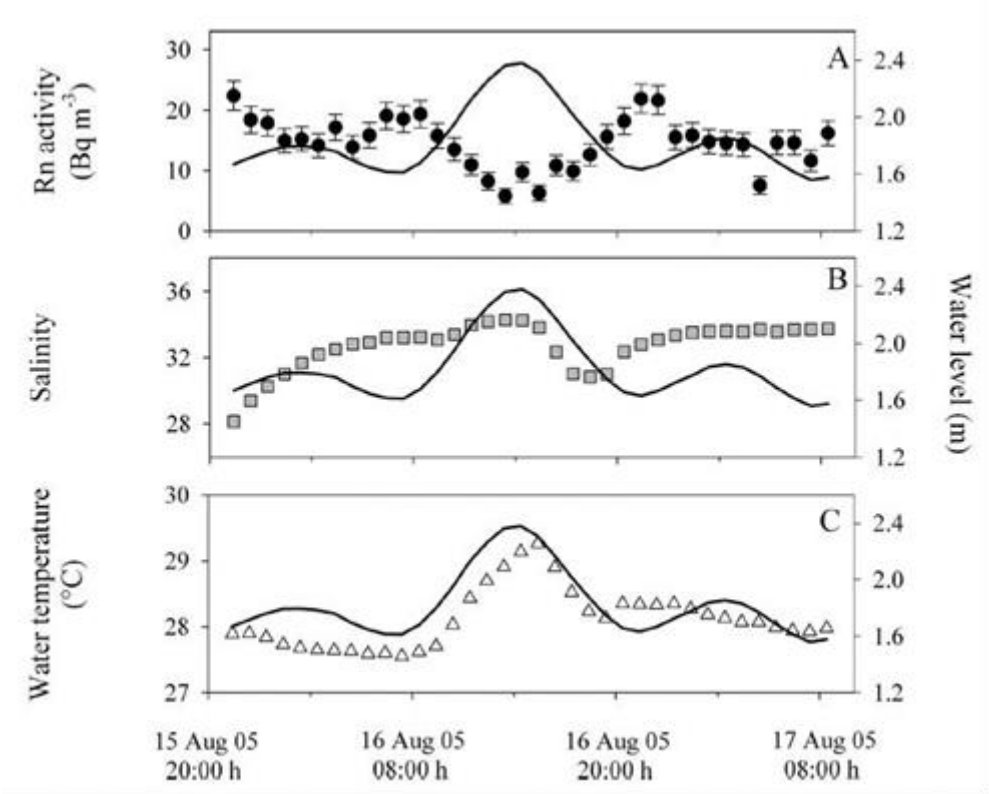

Figure 16. Time-series analysis of water properties in Kahauloa Bay surface plume water (Peterson et al., 2009)

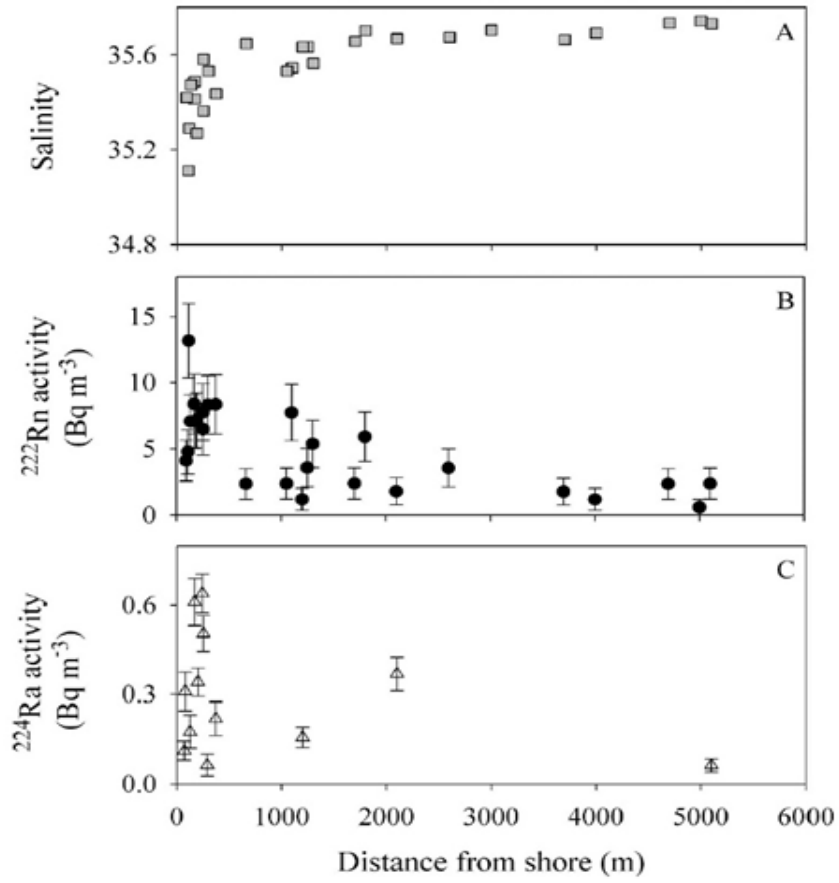

Figure 17. Longitudinal profile analysis of water properties in Kealakekua Bay offshore waters (Peterson et al., 2009)

With a naked eye, it can be seen how both plume water and source water are hotter than Mediterranean waters because of the tropical climate Hawaii region has, even though it is in the middle of the ocean. This precisely fact, being practically in the open sea, is what causes the aforementioned tidal process and the consequent mixing of the waters, which is why the difference between the salinities of the plume and oceanic offshore waters is much less than in the Torre Badum campaigns.

Peterson *et al.*, (2009) gives as result of the August 2006 campaign study an SGD flux in Kahauloa Bay of 1.100 m^3/day. Knowing the source salinity (S_{SGD}), FSGD flux can be obtained and is estimated to be 630 m^3/day, this is 0,23 Mm^3/year.

Meteorological data required, taken from the same website as previously named, is enlisted right below:

Meteorological Data	
Average atmosphere temperature on 7th August 2006, from 00:00 a.m. to 11:59 p.m. of the data campaign day	26 ºC
Daily average atmosphere temperature range on the data campaign day	7,6 ºC
Difference between the mean temperature of the hottest month (September) minus the mean temperature of the coldest month (February)	3,7 ºC
Hours of solar radiation on the data campaign day	14,18 hours (14 h and 11 min)
Precipitation on the data campaign day	1,74 mm/day (54 l/(m^2*month))
Cloudiness percentage on the data campaign day	48 %

Table 7. Meteorological data from Kahauloa Bay needed for the methodology, 7th August 2006 (source: climate-data.org)

Other data used in this article's methodologies is written below:

- The area covered by the SGD plume: 20.300 m^2 (0,0203 km^2)
- Offshore seawater temperature: 27,1 ºC
- Latitude of the source point at Kahauloa Bay: 19 º 27' 36'' N
- Altitude of the source point at Kahauloa Bay: 0m (obviously, at sea level)
- Length of the plume orthogonal to the coastline: 300 meters

- Width of the SGD source along the coastline: approximately 3 meters
- Width of the plume: approximately 1,2 meters

This time, the FSGD flux is quite smaller than the previous cases (1,2% of the October campaign flux and 0,04% of the subsequent June campaign flux). Once again, this will be another plus point to differentiate campaigns and see how the model develops with no similar characteristics from one case to another.

4.2. Adaptation for the method nº1

4.2.1. Definition of the geometry

Once the data collection is done, next step is to define how this data is used. As a reminder, Proposal nº1 consists of using the 'Submarine Outfalls' methodology. To do so, first we need to explain how to adapt formulae to our study case.

As explained before in section 2.3., the methodology considers a deeply submerged outfall. This means that the flux vector from source point directly upwards to the surface, while in our case we study mainly submarine horizontal discharges, having a movement vector with a huge horizontal component. For this reason, we considered to think our FSGD as a 2D horizontal problem, changing some concepts for the formulas.

Firstly, we saw previously how depending on the existence of vertical stratification, the initial factor of the methodology formula change (0,31 with stratification and 0,38 if it is a homogeneous media in terms of salinity). As our plume distributes and expands across the sea surface, the fact of having or not stratification should have no effect on the water movement, being able to consider it as a case with homogeneous salinity distribution along a vertical water column. Even so, both coefficients will be studied to draw conclusions with the two obtained results.

Secondly, the vertical distance component also varies (if there was no stratification we take 'd', vertical distance form source to surface, and if indeed there is stratification we need to consider 'y_{max}', vertical distance from source to depth where the plume reaches a salinity equilibrium with the ocean seawater). In our case, this distance will receive two different value options to analyze which fits better with the methodology and if there is a logical and rational explanation for it to fit or not. As said before, considering we have a horizontal 2D problem, we think vertical distance may take the value of the width of the plume (in the vertical direction) as well as the horizontal length of the plume.

With these clarifications, the used formulas are as follows:

$$S = K * \frac{g'^{1/3} * l}{q^{2/3}} \quad (8)$$

$$\text{with} \quad g' = g * \frac{\rho' - \rho}{\rho} \quad (9)$$

$$\text{with} \quad S = \frac{S_{sea}}{S_{fsgd}} \quad (10)$$

$$\text{with} \quad q = \frac{Q_{fsgd}}{w_{fsgd}} \quad (11)$$

S: centerline dilution [Ø]
K: stratification coefficient (0,31 or 0,38) [Ø]
g': modified gravitational acceleration [m/s^2]
l: vertical width or horizontal length of the plume [m]
q: initial discharge flow per unit length [m^2/s]
g: gravitational acceleration [m/s^2]
ρ': density of the ambient fluid [kg/m^3]
ρ: density of the discharged fluid [kg/m^3]
S_{sea}: seawater salinity [g/l]
S_{fsgd}: FSGD freshwater salinity [g/l]
Q_{fsgd}: FSGD freshwater flow [m^3/s]
w_{fsgd}: width of the FSGD source along the coastline [kg/m^3]

Isolating the variable in which we have interest, the final formula to calculate the total SGD flow is as follows:

$$Q_{fsgd} = \left(K * \frac{\left(g * \frac{\rho' - \rho}{\rho} \right)^{\frac{1}{3}} * l}{\left(\frac{S_{fsea}}{S_{fsgd}} \right)} \right)^{\frac{3}{2}} * w_{fsgd} \quad (12)$$

In the following Figure 18, it can be seen a geometric scheme of a plume with some of the equation's variables (case of l = horizontal length of the plume):

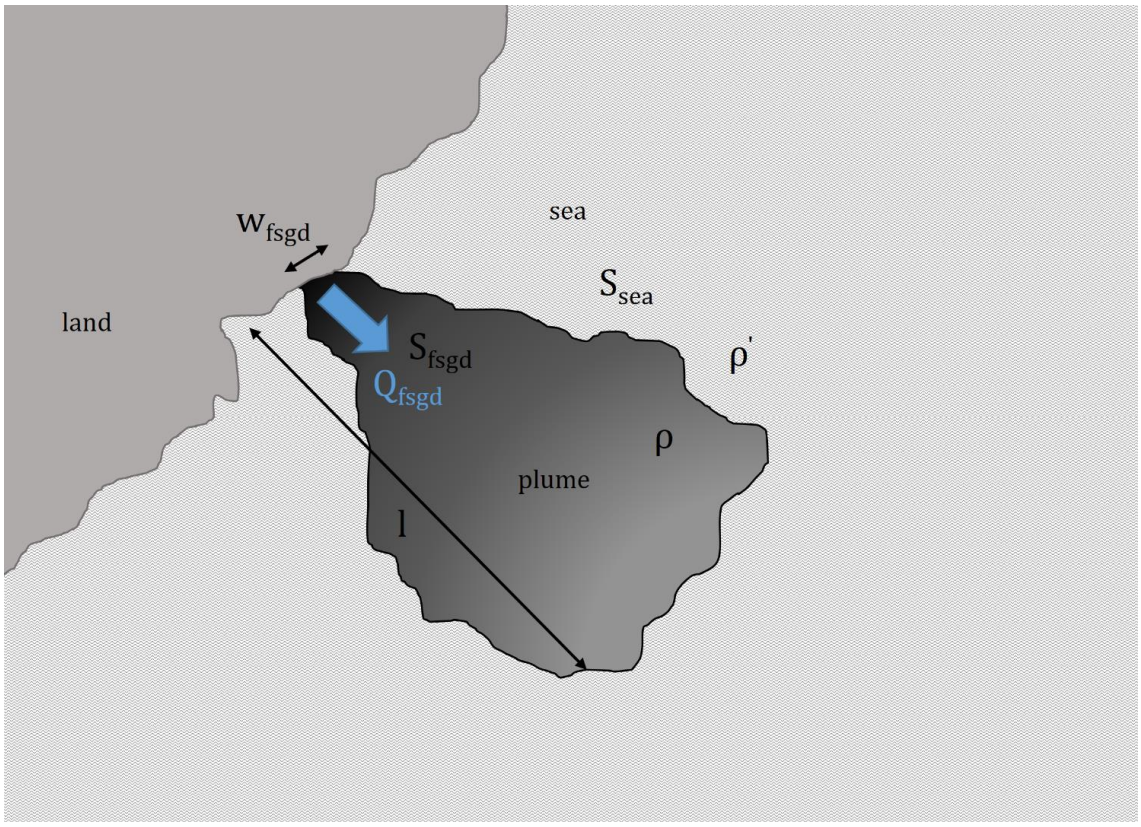

Figure 18. Geometric scheme of a plume and variables needed to solve the Submarine Outfalls' method formula.

4.3. Adaptation for the method nº2

4.3.1. Definition of the geometry

Regarding Proposal nº2, the Box Model methodology, its geometry is more complex than the previous one.

As briefly defined in section 2.5., this model is based on the subdivision of the estuary in compartments with almost same maritime properties (temperature (T), salinity (S), density (ρ), etc.), considering true the hypothesis of steady-state system (formulas 6 and 7).

Between this 'boxes' a series of flows are established. These are divided in two types: advective/convective flows and exchange/diffusive ones. A flow is defined as advective/convective when clean and direct transfer of water between two boxes takes place (this kind of flow tends to have horizontal direction, but it can also be vertical), while exchange/diffusive flows, also known as 'non-advective', are the ones that derive from turbulent diffusion between the boxes' water volumes, which means movement of the solutes between them (de Pedro, 2007).

To represent convective flows in our box model letter 'Q' will be used, while 'E' and 'F' letters will give name to salinity and heat diffusion flows, respectively. Every flow on the diagram is represented by its corresponding letter and two subindex numbers corresponding to the source

and destination compartment of the flow. As diffusion flows have predominant vertical direction, these ones would be included in our model.

In the following subsections, two possibilities for geometry considerations are exposed and explained.

In our study case, to meet the system of equations requirements and have as unknowns as the number of independent equations, we have also considered as a condition to be satisfied the heat (H) balance:

$$\frac{\delta H}{\delta t} = 0 \qquad (13)$$

This way, not only volume and salinity will affect on the fluxes, but also they will depend on temperature of water and atmosphere, applying a more restrictive level for the steady-state conditions.

4.3.1.1. Complex model

(de Pedro, 2007) considered up to 8 boxes to define its model, as he analyzed a system with 3 different inputs to his box model. As our study case consists only of one FSGD, this is one income flux, we can consider the same complex model with 3 boxes. The first one, named box nº1, is the plume itself, with salinity S_1 and temperature T_1. Box nº2 is the seawater body that stands right under the plume area, with salinity S_2 and temperature T_2. Last box, the third one, is defined as the body of water that contours boxes nº1 and nº2, connected with the open sea. In addition, other terms in the system need to be defined:

- The water exchange fluxes between two boxes consider both directions all summed up in one. This means that if there is a flux from (1) to (2), there is not another term that considers flux from (2) to (1). In this model, Q_{13}, Q_{32} and Q_{21} are the convective fluxes that have been considered, as well as E_{12} and F_{12} for the diffusion ones.
- In terms of mass balance, three other inputs to or outputs from box nº1, the plume, are considered: Q_{FSGD} is the inlet freshwater from the aquifer and discharged to the sea (the main unknown of our system), with physicochemical properties S_{FSGD} and T_{FSGD}; meteorological conditions also affect mass balance, with 'Precip.' and 'Evap.' as the precipitation and evaporation water fluxes entering and exiting the plume box, respectively.
- In terms of heat balance, the radiation striking the surface water also depends on meteorological conditions. This term is given the name 'Rad.'.

Once all this is taken into account, the following Figure 19 shows a proper scheme resuming all these previous definitions:

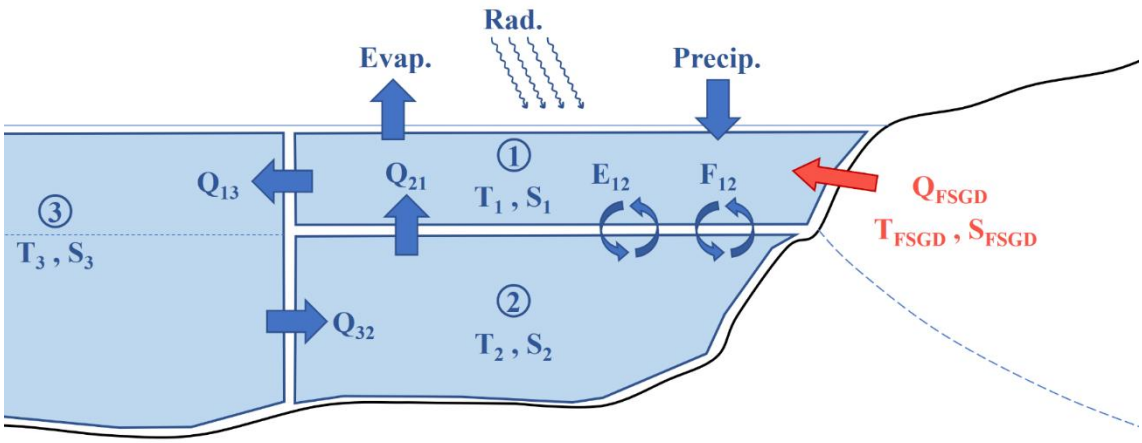

Figure 19. Complex box system, with all its corresponding variables to use for the 'box model' methodology

4.3.1.2. Simple model

Another possible approach to the problem is doing as (Peterson et al., 2009). On that article, they explain how it is possible to consider a simpler box model as in Figure 20, due to the contrast in some properties as salinity or isotopes activity, between open ocean water (high salinity and low isotopes activity) and the discharging groundwater (high isotopes activity and low salinity).

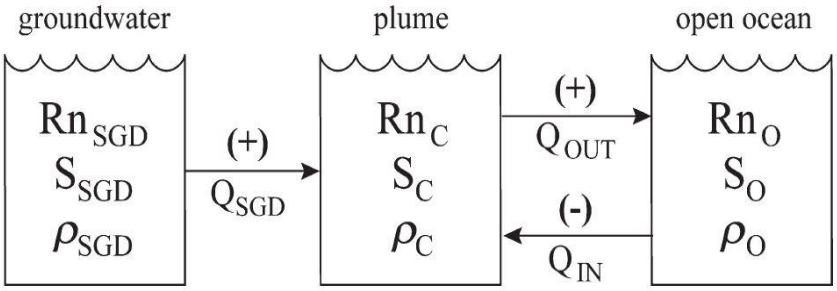

Figure 20. Simplified box model proposal from (Peterson et al., 2009)

Taking advantage of these properties gap, it is possible to analyze the output and input of fresh and saltwater flows to the intermediate box, which belongs to the so-called plume.

Considering then a new possible approach to the problem, taking diffusion terms as negligible, as well as merging boxes nº 2 and nº3, this lets a simplification of the problem with only 2 boxes: nº1 for the plume and box nº2 for the rest of the open sea saltwater. As in the previous subsection 4.3.1.1., these boxes have properties (S_1 , T_1) for box nº1 and (S_2 , T_2) for box nº2. At the end, as only two intern direct flows are considered, they only have one digit number subindex that refers to the box from which the flux exits (Q_1 for the flux from box nº1 to box nº2 and Q_2 for the opposite process). For the rest of variables, Q_{FSGD}, 'Precip.', 'Evap.' And 'Rad.', same considerations are taken into account.

The resulting scheme is resumed as follows:

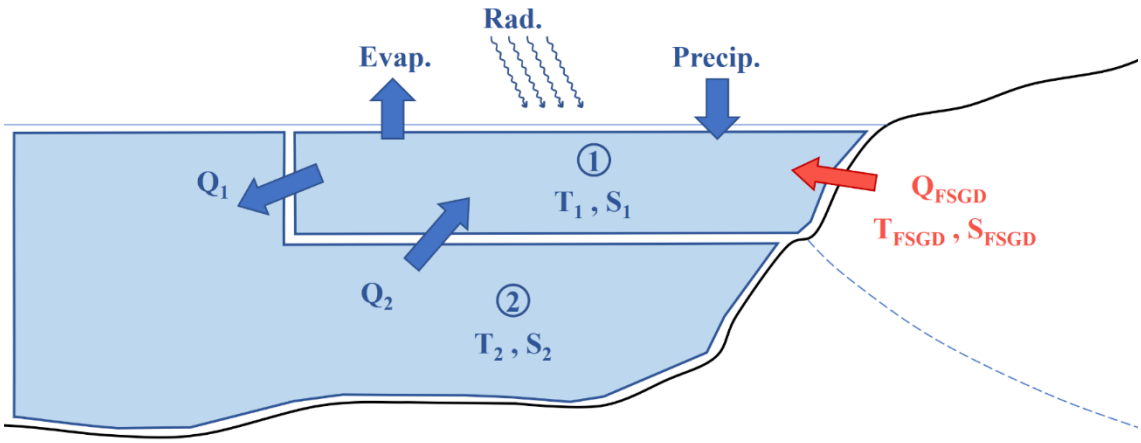

Figure 21. Simple box system, with all its corresponding variables to use for the 'box model' methodology

4.3.2. Definition of balance equations and variables

Once geometry is defined, the equation system needs to be defined with its formulas and variables. Equations 6, 7 and 13 show the three hypotheses that need to be taken into account for the model to be steady-state valid. To do so, in this section we are going to 'expand' those equations and analyze all their terms.

As two geometric options have been considered as possible proposals for the box model methodology, each one with a different level of complexity, also in terms of equations it will be necessary to distinguish between them. Complex model will be considered at first to define equations, to then explain the variations for the simple model.

4.3.2.1. Volume conservation equations

The first equation (nº6) is the volume conservation equation for boxes nº1 (plume) and nº2 (under the plume). On them, convective flows of direct water entering or exiting the boxes are considered (as a general rule, flows that enter a box are considered as positive terms in the equation). Adding also the meteorological fluxes, these equations are as follows:

(1) $$Q_{21} + Q_{FSGD} + Precip. = Q_{13} + Evap. \quad (14)$$

(2) $$Q_{32} = Q_{21} \quad (15)$$

Q_{21}: water flux from box nº2 to box nº1 [m^3/day] (unknown)
Q_{FSGD}: water flux from aquifer to box nº1 [m^3/day] (main unknown)
$Precip.$: rain water over box nº1 surface [m^3/day] (DATA)
Q_{13}: water flux from box nº1 to box nº3 [m^3/day] (unknown)
$Evap.$: evaporation water from box nº1 surface [m^3/day]

Q_{32}: water flux from box nº3 to box nº2 [m^3/day] (unknown)

Evaporation data can't be directly obtained. Instead, it is provided by the '*Penman Equation*' (Linacre, 1977):

$$E = \frac{m * R_n + \rho_a * c_p * \delta_e * g_a}{\lambda_v * (m + \gamma)} \quad (16)$$

redistributing,

$$E = \frac{R_n + \rho_a * c_p * \frac{\delta_e}{m} * g_a}{\lambda_v * \left(1 + \frac{\gamma}{m}\right)} \quad (17)$$

E: Penman's evaporation rate [g/(cm^2*s)]
R_n: net radiation [cal/(cm^2*s)]
ρ_a: air density = 1,3*10^{-3} g/cm^3
c_p: heat capacity of air = 0,24 cal/(g*ºC)
δ_e: vapor pressure deficit [Pa]
m: slope of the 'saturation vapor pressure' curve [Pa/ºC]
g_a: moment of surface aerodynamic conductance = 0,8$\hat{3}$ cm/s
λ_v: latent heat of vaporization = 580 cal/g
γ: psychrometric constant = 0,67 mbar/ºC

The net radiation term, R_n, derives from another formula with terms from other empirical expressions:

$$R_n = (0{,}75 - \alpha) * Q_s \quad (18)$$

with $$Q_s = \frac{T_m}{60 * (100 - A)} \quad (19)$$

and $$T_m = T + 6 * 10^{-5} * h \quad (20)$$

α: ocean albedo = 0,06 = 6%
Q_s: global-radiation flux-intensity for cloudless and overcast conditions [cal/(cm^2*s)]
T_m: sea-level equivalent of the measured mean temperature [ºC]
A: latitude of the study site [º] (DATA)
T: atmosphere mean temperature [ºC] (DATA)
h: elevation / altitude [cm] (DATA)

The terms $\frac{\delta_e}{m}$ and $\left(1+\frac{\gamma}{m}\right)$ are replaced by equivalent expressions that depends only on temperature values. On one side, Figure 22 shows the relationship between an analytical expression and $\left(1+\frac{\gamma}{m}\right)$, of almost equal values (less than 0,1 error) when T ϵ [8 ºC , 36 ºC]. So, the new empirical expression is:

$$\left(1+\frac{\gamma}{m}\right) = 2 * (1 - 0{,}0125 * T) \qquad (21)$$

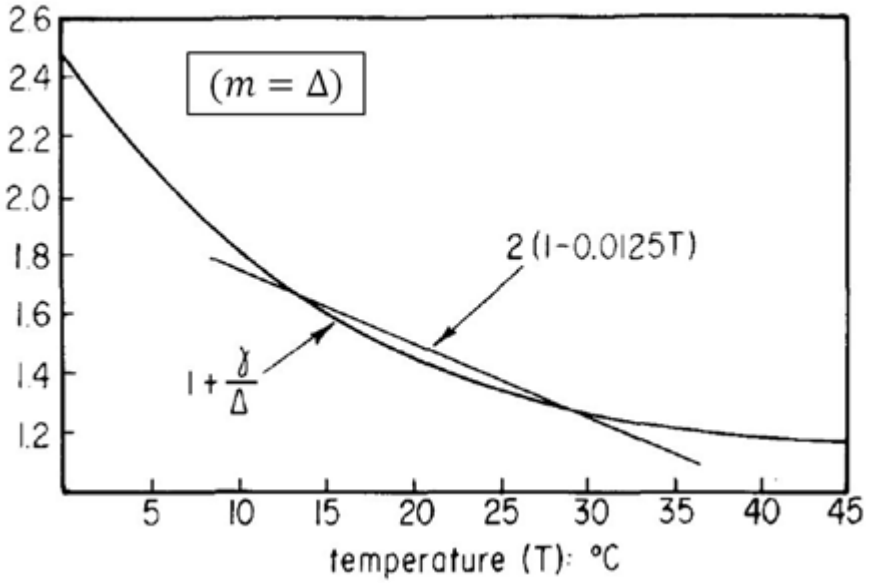

Figure 22. Relationship between a Penman's equation term and an only temperature-dependent expression (Linacre, 1977)

On the other side, $\frac{\delta_e}{m}$ can also be substituted by other empirical expressions written here below:

$$\frac{\delta_e}{m} = T - T_d \qquad (22)$$

with $$T - T_d = 0{,}0023 * h + 0{,}37 * T + 0{,}53 * R + 0{,}35 * R_{ann} - 10{,}9\ ºC \qquad (23)$$

T_d: dew-point temperature [ºC]
R: mean daily range temperature [ºC] (DATA)
R_{ann}: difference between the mean temperatures of the hottest and coldest months [ºC] (DATA)

Equation 23 will be valid and assumed as true only if precipitation is at least 5 mm/month and the result of $T - T_d$ is greater than 4 ºC.

With all the previous statements, the final expression of $Evap.$ is:

$$Evap. = 3{,}6 * 10^4 * \frac{E * Ar * T_{rad}}{\rho_w} \quad (24)$$

Ar: surface area of study site (plume) [m^2] (DATA)
T_{rad}: effective radiation day hours [h/day] (DATA)
ρ_w: water density = 1.000 g/dm^3

4.3.2.2. Salt conservation equations

The second steady-state condition equations are the salt conservation equation for boxes nº1 (plume) and nº2 (under the plume). On them, both convective flows of direct water entering or exiting the boxes and diffusive flows of dissolved solutes are considered:

(1) $$S_2 * (Q_{21} + E_{12}) + S_{FSGD} * Q_{FSGD} = S_1 * (Q_{13} + E_{12}) \quad (25)$$

(2) $$S_3 * Q_{32} + S_1 * E_{12} = S_2 * (Q_{21} + E_{12}) \quad (26)$$

S_2: salinity of box nº2 [g/l] ≡ [‰] (DATA)
E_{12}: diffusion solute flux between box nº1 and box nº2 [m^3/day] (unknown)
S_{FSGD}: salinity of the aquifer [g/l] ≡ [‰] (DATA)
S_1: salinity of box nº1 [g/l] ≡ [‰] (DATA)
S_3: salinity of box nº3 [g/l] ≡ [‰] (DATA)

4.3.2.3. Heat conservation equations

The third and last condition equation (equation 13) is the heat conservation equation, applied again on boxes nº1 (plume) and nº2 (under the plume). Adding the radiation heat input, these equations are as follows:

defining $H_i = \rho_i * c_i * (T_i + 273{,}15)$, then we have (27)

(1) $$H_2 * (Q_{21} + F_{12}) + H_{FSGD} * Q_{FSGD} + Rad. = H_1 * (Q_{13} + F_{12}) \quad (28)$$

(2) $$H_3 * Q_{32} + H_1 * F_{12} = H_2 * (Q_{21} + F_{12}) \quad (29)$$

ρ_i: density of the 'i-box' (i = 1, 2, 3, FSGD) [kg/m^3]
c_i: specific heat of the 'i-box' (i = 1, 2, 3, FSGD) [J/(kg*K)]
T_i: water temperature in the 'i-box' (i = 1, 2, 3, FSGD) [ºC] (DATA)
F_{12}: diffusion heat flux between box nº1 and box nº2 [m^3/day] (unknown)
$Rad.$: radiation received on the box nº1 surface [J/day]

Density variables can be obtained with the state equation of (UNESCO, 1980). Assuming a standard atmosphere (P=0), the density of a body of water can be determined from temperature and salinity as:

$$\rho(S,T,0) = A + B * S + C * S^{3/2} + D * S^2 \quad (30)$$

with

$$A = a_0 + a_1 * T + a_2 * T^2 + a_3 * T^3 + a_4 * T^4 + a_5 * T^5 \quad (31)$$

$$B = b_0 + b_1 * T + b_2 * T^2 + b_3 * T^3 + b_4 * T^4 \quad (32)$$

$$C = c_0 + c_1 * T + c_2 * T^2 \quad (33)$$

$$D = d_0 \quad (34)$$

$$a_0 = 999{,}842594 \qquad b_0 = 8{,}22493 * 10^{-1} \qquad c_0 = -5{,}72466 * 10^{-3}$$

$$a_1 = 6{,}793952 * 10^{-2} \qquad b_1 = -4{,}0899 * 10^{-3} \qquad c_1 = 1{,}0227 * 10^{-4}$$

$$a_2 = -9{,}095290 * 10^{-3} \qquad b_2 = 7{,}6438 * 10^{-5} \qquad c_2 = -1{,}6546 * 10^{-6}$$

$$a_3 = 1{,}001685 * 10^{-4} \qquad b_3 = -8{,}2467 * 10^{-7} \qquad d_0 = 4314 * 10^{-4}$$

$$a_4 = -1{,}120083 * 10^{-6} \qquad b_4 = 5{,}3875 * 10^{-9}$$

$$a_5 = 6{,}536332 * 10^{-9}$$

Specific heat variables can be obtained by using a similar equation scheme from (Sharkawy *et al.*, 2010):

$$c = A + B * T + C * T^2 + D * T^3 \quad (35)$$

with

$$A = a_0 + a_1 * S + a_2 * S^2 \quad (36)$$

$$B = b_0 + b_1 * S + b_2 * S^2 \quad (37)$$

$$C = c_0 + c_1 * S + c_2 * S^2 \quad (38)$$

$$D = d_0 + d_1 * S + d_2 * S^2 \quad (39)$$

$$a_0 = 5{,}328 \qquad c_0 = 9{,}6 * 10^{-6}$$

$$a_1 = -9{,}76 * 10^{-2} \qquad c_1 = -1{,}927 * 10^{-6}$$

$$a_2 = 4{,}04 * 10^{-4} \qquad c_2 = 8{,}23 * 10^{-9}$$

$$b_0 = -6{,}913 * 10^{-3} \qquad d_0 = 2{,}5 * 10^{-9}$$

$$b_1 = 7{,}351 * 10^{-4} \qquad d_1 = 1{,}666 * 10^{-9}$$

$$b_2 = -3{,}15 * 10^{-6} \qquad d_2 = -7{,}125 * 10^{-12}$$

The $Rad.$ term cannot be directly obtained. Instead, radiation data is provided by the '*Mosby Equation*' (Varela and Rosón, 2008), which before needs to know the value of the following six terms. First, we start calculating the insolation with a totally clear sky:

$$Q_s^{clear} = 0{,}73 * \left[222 + 772 * sin^2\left(\frac{\pi * (12 - M)}{12}\right)\right] \quad (40)$$

Q_s^{clear}: clear sky insolation/radiation [cal/(cm²*day)]
M: month of campaign number (January = 1, February = 2, etc.) (DATA)

Second, to obtain the real radiation that hits the sea surface, a correction factor due to the cloudiness needs to be taken into account:

$$Q_s^{hits} = Q_s^{clear} * (1 - 0{,}007 * N) \quad (41)$$

Q_s^{hits}: modified radiation by cloudiness factor [cal/(cm²*day)]
N: cloudiness percentage on the total celestial (DATA)

In third place, the radiation that actually penetrates the surface and enters the hypothetical box is:

$$Q_s^{input} = Q_s^{hits} * (1 - \alpha) \quad (42)$$

Q_s^{input}:modified radiation by the reflex albedo factor [cal/(cm²*day)]
α: ocean albedo = 0,06 = 6%

Then, the next step is to calculate the ocean background radiation minus the one of the atmosphere. The following formula considers both sea and atmosphere as perfect black bodies, and positive values mean sea receiving heat:

$$Q_b = (\sigma * 2{,}3885 * 10^{-5}) * ((T_{air} + 273{,}15)^4 - (T_{ss} + 273{,}15)^4) \quad (43)$$

Q_b: total background radiation [cal/(cm²*day)]
σ: the Stephan-Boltzmann constant = 5,67*10^{-8} W/(m²*K⁴)
T_{air}: atmosphere air temperature [ºC] (DATA)
T_{ss}: sea surface temperature [ºC] (DATA)

Following, the calculation of the heat losses caused by water evaporation is also necessary for the overall results:

$$Q_e = -\lambda * \left(10^2 * \frac{Evap.}{Ar}\right) \quad (44)$$

Q_e: evaporation heat loss [cal/(cm²*day)]

λ: latent heat of evaporation = 550 cal/cm^3

$Evap.$: evaporation water from box nº1 surface [m^3/day]

Ar: surface area of study site (plume) [m^2] (DATA)

The last of the six factors is the radiation produced by the heat conduction between air and water, which depends on the temperature gap between them. In the following formula, positive values mean sea receiving heat:

$$Q_h = d_{air} * Cp_{air} * D_h * (T_{air} - T_{ss}) * (3{,}6 * 10^3 * T_{rad}) \quad (45)$$

Q_h: heat conduction flux [cal/(cm^2*day)]

d_{air}: atmosphere air density = 1,1989*10^{-3} g/cm^3

Cp_{air}: specific heat of the atmosphere air = 0,24 cal/(g*ºC)

D_h: heat transfer coefficient = 0,5 cm/s

T_{rad}: effective radiation day hours [h/day] (DATA)

All these radiation components are represented in the following Figure 23:

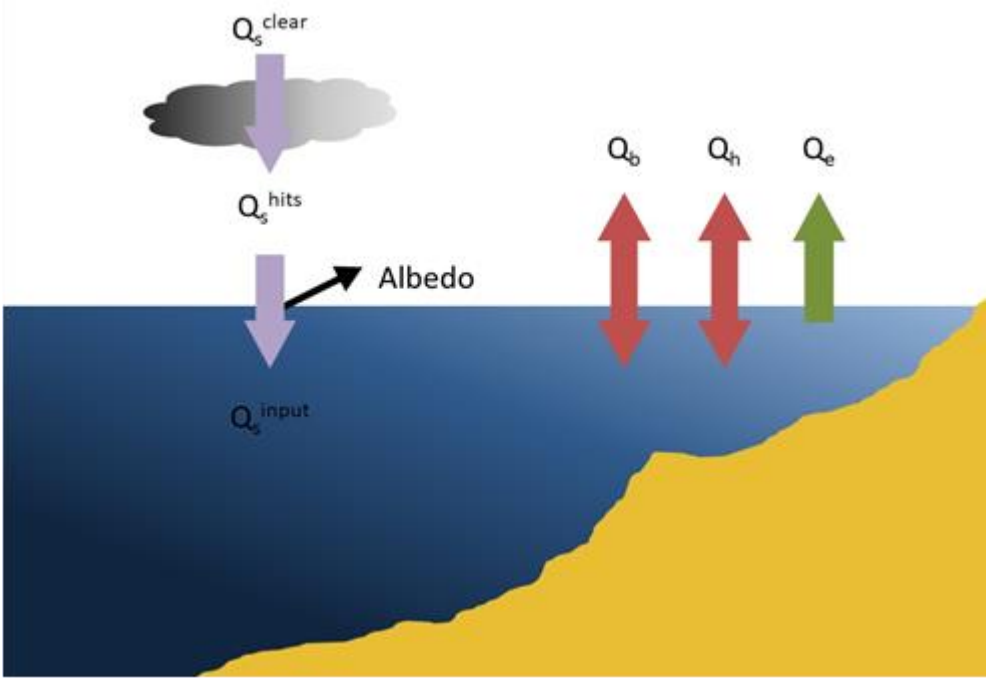

Figure 23. Radiation decomposition by terms, modified from (Varela and Rosón, 2008)

Finally, the $Rad.$ term to complete the 'heat conservation equation' can be obtained by the next 2 equations:

$$Rad. = 4{,}184 * 10^{-4} * Q_t * Ar \quad (46)$$

with $Q_t = Q_s^{input} + Q_b + Q_e + Q_h$ (47)

Q_t: sea total radiation input per unit of surface area [cal/(cm²*day)]

4.3.2.4. Simple model variation

For the simple model, the fact that there are only two boxes simplifies a lot the system of equations. Instead of applying each of the three hypotheses in two boxes, they are applied only once in box nº1 (the one of the plume). In this case, diffusive fluxes are not considered, and the convective fluxes' subindex define their origin (this means that Q_1 is the flux from box nº1 to box nº2). Positive sense of the variables stays the same, as well as all the other considerations taken into account for the complex model. The new system of equations is written down below:

(1) $$Q_2 + Q_{FSGD} + Precip. = Q_1 + Evap. \quad (48)$$

(1) $$S_2 * Q_2 + S_{FSGD} * Q_{FSGD} = S_1 * Q_1 \quad (49)$$

(1) $$H_2 * Q_2 + H_{FSGD} * Q_{FSGD} + Rad. = H_1 * Q_1 \quad (50)$$

where $$H_i = \rho_i * c_i * (T_i + 273{,}15) \quad (51)$$

Q_2: water flux from box nº2 to box nº1 [m³/day] (unknown)
Q_{FSGD}: water flux from aquifer to box nº1 [m³/day] (main unknown)
$Precip.$: rainwater over box nº1 surface [m³/day] (DATA)
Q_1: water flux from box nº1 to box nº2 [m³/day] (unknown)
$Evap.$: evaporation water from box nº1 surface [m³/day]
S_2: salinity of box nº2 [g/l] ≡ [‰] (DATA)
S_{FSGD}: salinity of the aquifer [g/l] ≡ [‰] (DATA)
S_1: salinity of box nº1 [g/l] ≡ [‰] (DATA)
ρ_i: density of the 'i-box' (i = 1, 2, FSGD) [kg/m³]
c_i: specific heat of the 'i-box' (i = 1, 2, FSGD) [J/(kg*K)]
T_i: water temperature in the 'i-box' (i = 1, 2, FSGD) [ºC] (DATA)
$Rad.$: radiation received on the box nº1 surface [J/day]

4.3.3. Definition of the matrix problem

Once the systems' equations are defined, we have two matrix problems. The complex model consists of a system of six equations and six unknowns (Q_{FSGD}, Q_{13}, Q_{21}, Q_{32}, E_{12} and F_{12}). By solving this problem, the five 'inter-boxes' fluxes will have their values but what draw most of our attention is the Q_{FSGD} term, the freshwater discharge from the aquifer to the sea, the main objective to solve in this project.

Grouping the equations coefficients and the constant values in an augmented matrix, we have:

$$\begin{bmatrix} 1 & -1 & 1 & 0 & 0 & 0 \\ 0 & 0 & 1 & -1 & 0 & 0 \\ S_{FSGD} & S_1 & S_2 & 0 & S_2 - S_1 & 0 \\ 0 & 0 & -S_2 & S_3 & S_1 - S_2 & 0 \\ H_{FSGD} & H_1 & H_2 & 0 & 0 & H_2 - H_1 \\ 0 & 0 & -H_2 & H_3 & 0 & H_1 - H_2 \end{bmatrix} \begin{bmatrix} Evap. - Precip \\ 0 \\ 0 \\ 0 \\ -Rad. \\ 0 \end{bmatrix}$$

$$Q_{FSGD} \quad Q_{13} \quad Q_{21} \quad Q_{32} \quad E_{12} \quad F_{12}$$

By changing the equations system to a matrix system, the resultant (6x6) problem to solve is the following:

$$\begin{bmatrix} 1 & -1 & 1 & 0 & 0 & 0 \\ 0 & 0 & 1 & -1 & 0 & 0 \\ S_{FSGD} & -S_1 & S_2 & 0 & S_2 - S_1 & 0 \\ 0 & 0 & -S_2 & S_3 & S_1 - S_2 & 0 \\ H_{FSGD} & -H_1 & H_2 & 0 & 0 & H_2 - H_1 \\ 0 & 0 & -H_2 & H_3 & 0 & H_1 - H_2 \end{bmatrix} * \begin{bmatrix} Q_{FSGD} \\ Q_{13} \\ Q_{21} \\ Q_{32} \\ E_{12} \\ F_{12} \end{bmatrix} = \begin{bmatrix} Evap. - Precip \\ 0 \\ 0 \\ 0 \\ -Rad. \\ 0 \end{bmatrix}$$

Applying the same process to the simple model, the resulting (3x3) matrix system to solve is written down below:

$$\begin{bmatrix} 1 & -1 & 1 \\ S_{FSGD} & -S_1 & S_2 \\ H_{FSGD} & -H_1 & H_2 \end{bmatrix} * \begin{bmatrix} Q_{FSGD} \\ Q_1 \\ Q_2 \end{bmatrix} = \begin{bmatrix} Evap. - Precip \\ 0 \\ -Rad. \end{bmatrix}$$

4.4. Calculations

According to algebraic fundamentals, a matrix system $\overline{\overline{A}} * \bar{x} = \bar{b}$ (the coefficients matrix, the unknown vector and the constants vector, respectively), where A dimensions are (m x n) and m = n (this means that there is the same amount of unknowns than equations), and there are no dependent rows/columns in such matrix, then the system can be solved by the following calculations:

$$\text{if:} \quad \overline{\overline{A}} * \bar{x} = \bar{b}$$

$$\text{then:} \quad \left(\overline{\overline{A}}\right)^{-1} * \overline{\overline{A}} * \bar{x} = \left(\overline{\overline{A}}\right)^{-1} * \bar{b}$$

$$\bar{x} = \left(\bar{\bar{A}}\right)^{-1} * \bar{b}$$

$\left(\bar{\bar{A}}\right)^{-1}$: the inverse of the coefficient's matrix, $\bar{\bar{A}}$

This simple process to invert a matrix and multiply the resultant matrix by a vector can be done either with the MATLAB software or with the Microsoft Excel program. Both computational tools are easy to use and provide instantly results. In our study, we have chosen to use Microsoft Excel because of the additional ease it provides in organizing, manipulating and operating the necessary data, gathered from the sources already named.

Once the calculus is done, we proceed to analyze them in the following section 5.

5. RESULTS

5.1. Method's Testing: Castellón (October 2006)

Although our system of equation is capable of giving also fluxes between boxes, the truth is that these values cannot be analyzed if they are reasonable because there is no data to stick to. Instead, as previously seen in chapter 4.1.1.1. ('Ocean and meteorological data'), the studies in which we base our methodologies analysis give an estimation of the source discharge flux from the aquifer to the ocean. In the October 2006 campaign study of the Torre Badum's SGD plume, the freshwater discharge flux is claimed to be 50.500 m^3/day.

5.1.1. 'Submarine Outfalls'

First, we used methodology nº1 of the submarine outfalls, the simpler and easier one. By substituting the variables with their values, four possible scenarios are studied:

i) homogeneous salinity profile + distance equals to vertical width of the plume
ii) homogenous salinity profile + distance equals to horizontal length of the width
iii) stratified salinity profile + distance equals to vertical width of the plume
iv) stratified salinity profile + distance equals to horizontal length of the width

The table below shows the resulting FSGD flow for each of the four scenarios:

FSGD RESULTS (reference: 50.000 m^3/day)		
	l = vertical plume width	l = horizontal plume length
Non-stratified profile	i) 38.922,98 m^3/day	ii) 63.956,98 * 10^5 m^3/day
Stratified profile	iii) 28.679,61 m^3/day	iv) 47.125,41 * 10^5 m^3/day

Table 8. Results on Torre Badum's October campaign with Submarine Outfalls methodology

At first, it can already be seen how there are substantial differences between the results considering one value for l or another. There are 5 orders of magnitude separating the FSGD flow considered as correct and the solution numbers when considering l as the horizontal length of the plume. This confirms that taking this assumption is not correct at all and is immediately discarded from our proposals to apply to other study cases. Focusing now the analysis on the case where l takes the value of the plume's thickness, regarding the other assumption about the stratification of the vertical profile of the plume zone, both results are within the same order of magnitude of the 50.000 m^3/day, but they still clearly differ. Non-stratified case resulting flux (38.922,98 m^3/day) is 23% smaller than the expected solution, while stratified case (28.679,61 m^3/day) is even less accurate as it is almost half of the expected flow, with a 56% of accuracy.

Even if the results are not quite good in the first study case, this methodology will continue to be tested in the following scenarios to confirm or reject what is obtained in the first instance and to better calibrate the precision percentages.

5.1.2. Complex 'Box Model'

Leaving methodology nº1 for now and moving on to nº2, the result of the complex box model will be analyzed in first place. After building the calculus file, introducing formulas and values, we obtain the following resulting vector for the internal and input water fluxes:

$$\bar{x} = \begin{bmatrix} Q_{FSGD} \\ Q_{13} \\ Q_{21} \\ Q_{32} \\ E_{12} \\ F_{12} \end{bmatrix} = \begin{bmatrix} -219.364{,}511 \\ -612.592{,}090 \\ -392.722{,}305 \\ -392.722{,}305 \\ -47.671{,}494 \\ -326.621{,}936 \end{bmatrix} \; [m^3/day]$$

Negative values indicate an incorrect assumption of the direction of the flows, meaning the origin and destination boxes must be reversed (in Figure 24 it can be seen the scheme with corrected fluxes). Even so, not only does the sign not leave us good feelings regarding this model, but the flow of the submarine groundwater discharge, 219.364,511 m^3/day, is more than 4 times the expected flow (50.000 m^3/day).

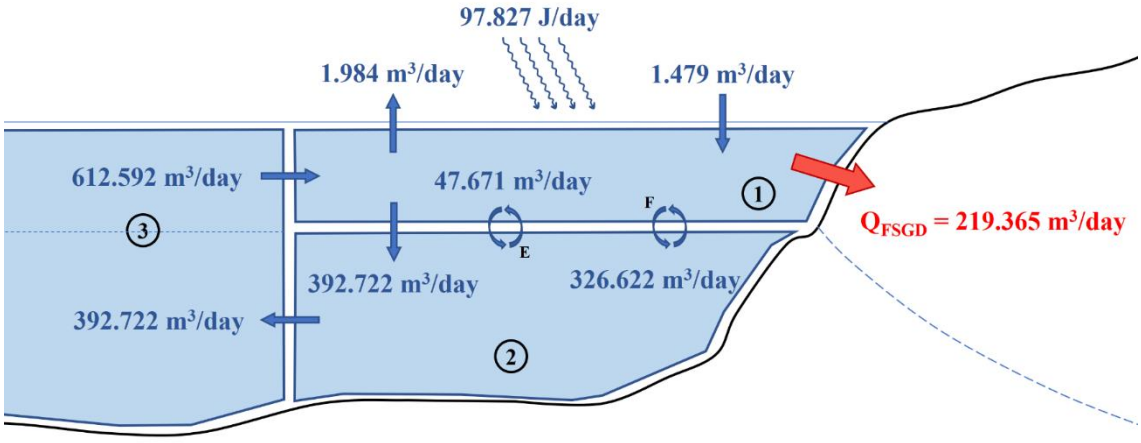

Figure 24. Solution to the box model 6x6 system in Torre Badum's October campaign, with its fluxes

Once again, it is considered convenient to eliminate this model from the analysis with the rest of the scenarios, since the sign of the results is meaningless. Later, in chapter 7. Discussion and Conclusions, the possible causes of these results will be analyzed, as well as the methodology of submarine outfalls using the length of the plume as the distance traveled by the discharge, as said in the previous point.

5.1.3. Simple 'Box Model'

Once the complex model has been tested, it's moment to analyze the results of the simpler variation of the model. This time, de 3x3 equation system gives the following resulting vector for the internal and input water fluxes:

$$\bar{x} = \begin{bmatrix} Q_{FSGD} \\ Q_1 \\ Q_2 \end{bmatrix} = \begin{bmatrix} 33.656{,}007 \\ 98.797{,}969 \\ 65.647{,}237 \end{bmatrix} \quad [m^3/day]$$

This time at least the values sign coincides with our hypothesized fluxes' sense. The results, although they do not show a very high level of precision, greatly reinforce the simple model, since its functionality has not yet been ruled out and gives hope to be able to carry out a good calibration of this methodology. The order of magnitude of the Q_{FSGD} flux matches with the solution (order of magnitude 4). With respect to the other inter-box fluxes, Q_1 and Q_2 , even if there's no data to compare them with their values are completely reasonable, since their orders of magnitude do not vary or do not vary much with respect to the FSGD flux. In Figure 25 this solution scheme is represented.

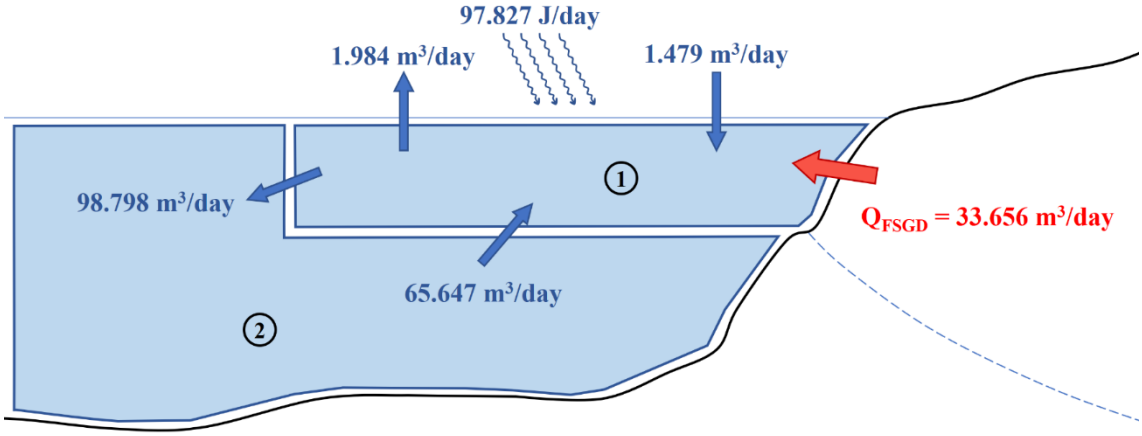

Figure 25. Solution to the box model 3x3 system in Torre Badum's October campaign, whit its fluxes

Similarly to the methodology nº1 results that have not been yet rejected, this simple box model gives, in this first data campaign at Torre Badum, a level of accuracy of 67% with respect to the 50.000 m^3/day given by (García-Solsona, 2010), good number for our method testing project to start with.

5.2. Validation of the Results

After testing all the proposed methodologies with their different proposals and variations, and after having thought it is not appropriate to go ahead with some of them, with others instead, hopeful results have been obtained with which to continue checking their ability to adapt to new cases and to give answers to the main problem of this project, the 'unknown' fluxes from aquifers in SGD plumes. In the following subchapters 6.1. to 6.4., the obtained results will be explained.

This time only results from the two non-discarded methodologies will be explained in detail, even though refused methods have been used again to reaffirm the falsity of their resulting values.

5.2.1. 'Submarine Outfalls' check in Castellón (June 2007)

As said before, (García-Solsona, 2010) carried out two data campaigns at the same site in Torre Badum. The second one took place 8 months after the first one, with seasonal characteristics opposite to the ones in October, with respect to ocean and meteorological conditions. From the data obtained with the sampling in the 2007's summer, the study determines a flow in the discharge source of approximately 159.400 m^3/day, more than three times higher than in the previous case.

For the submarine outfalls' methodology, after substituting the variables with their values, considering only the scenarios i) and iii) seen previously in chapter 5.1.1., the obtained results are shown in the table below:

FSGD RESULTS (reference: 159.400 m^3/day)		
	l = vertical plume width	
Non-stratified profile	i)	28.983,91 m^3/day
Stratified profile	iii)	21.356,21 m^3/day

Table 9. Results on Torre Badum's June campaign with Submarine Outfalls methodology

It is obvious that this time the numbers are far from the precision that has been obtained in the autumn campaign. Both solutions have decreased compared to the ones from table 8 when the real flow has in fact increased, leaving low percentages of similarity between the theoretical and the real fluxes (18% of similarity for the case of the non-stratified profile and 13% for the stratified one).

Although this method seems to perish, it is still way better than the rejected hypothesis that considers l as the horizontal plume's length, that is still 4 orders of magnitude lower.

5.2.2. 'Box Model' check in Castellón (June 2007)

To evaluate again the Box Model methodology, this time with the June data campaign, only the simple model will be used in to analyze its functionality. Even though, before completely rejecting the complex model, it has been tested with this case and has repeated with incongruent results, giving negative flow values and not being reasonable to the reference FSGD flux value. Instead, the 3x3 system gets solved by the same process as in the October campaign and still give optimistic results.

After adding new values to the formulas in the calculus file, we obtain the following resulting vector for the internal and input water fluxes:

$$\bar{x} = \begin{bmatrix} Q_{FSGD} \\ Q_1 \\ Q_2 \end{bmatrix} = \begin{bmatrix} 215.746{,}272 \\ 542.272{,}255 \\ 329.093{,}949 \end{bmatrix} \quad [m^3/day]$$

Contrary to what was obtained in point 5.1.3, the flows obtained differ upwards with respect to the theoretical FSGD flux on which the model is based, 159,400 m^3/day, although the order of magnitude matches with the solution (order of magnitude 5) In more detail, the 215.746 m^3/day is a flux about 35% higher than the expected one, being too high to be considered a good level of accuracy, but still provides quite encouraging data for this method. In Figure 26 the solution scheme is shown:

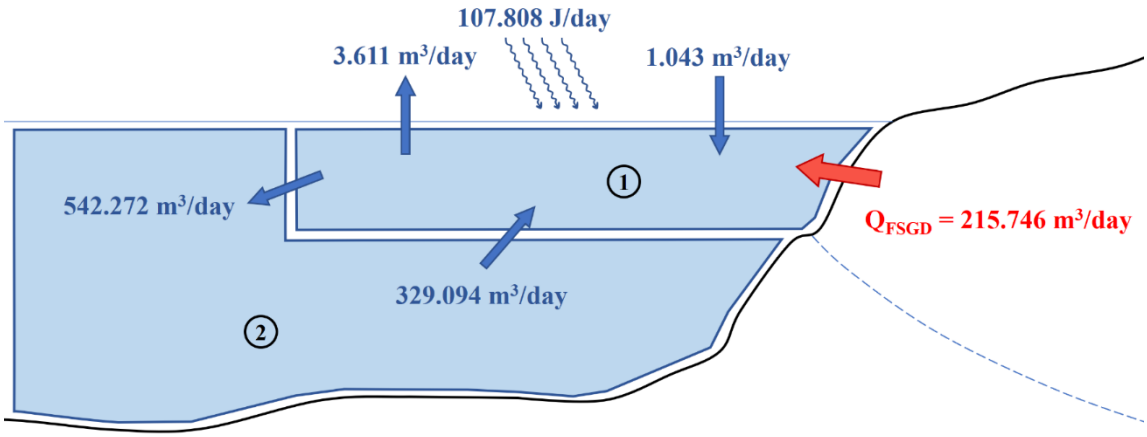

Figure 26. Solution to the box model 3x3 system in Torre Badum's Juner campaign, whit its fluxes

So far, results for both GDS flows have been obtained in the study by (Garcia-Solsona, 2010). Neither has approached the theoretical reference value with high accuracy, one has fallen short and the other has passed, although if we calculate the average of the similarities in the October and June campaigns (67% and 135%, respectively), we are left with an average accuracy value of 101%, which is very positive.

5.2.3. 'Submarine Outfalls' check in Hawaii

At this point, both campaigns at Torre Badum have been useful to test the reliability on our study methodologies, by applying the data collected from two completely opposite seasons of the year in terms of the relevant maritime characteristics of these models. To further explore new scenarios where these models can be applied, not only 'same site, varying campaign' must be considered, but also 'site diversity' must be a mandatory phase of the method evaluation. To carry out this requirement, we have come across (Peterson *et al.*, 2009) study in Hawaii Big Island's west coast, providing a perfect contrast point of view with a ocean system completely divergent compared to the one in Castellón.

From the data obtained with the data from August 2006, the study determines a flow in the discharge source of approximately 630 m^3/day, significantly smaller than the previous two FSGD fluxes (-98,75% and -99,60%, respectively).

For the submarine outfalls' methodology, by applying the corresponding data and not-rejected scenarios, the obtained results are shown in the table below:

FSGD RESULTS (reference: 630 m^3/day)		
	l = vertical plume width	
Non-stratified profile	i)	3.048,76 m^3/day
Stratified profile	iii)	2.246,42 m^3/day

Table 10. Results on Kahauloa Bay's August campaign with Submarine Outfalls methodology

Opposite from what obtained in the Torre Badum's June campaign, these results are much bigger than the expected theoretical values. Again, these numbers are far from the precision that has been obtained in the autumn campaign, but now both accuracy percentages have increased compared to the ones from October campaign, with growth rates between the theoretical and the real fluxes of about 384% for the non-stratified profile case and 257% for the stratified one (this is, almost 4 and 2,5 times the 630 m^3/day solution given in the Hawaii study).

5.2.4. 'Box Model' check in Hawaii

The last data check was performed using the Simple Box model with Hawaii's campaign. Once more, the 3x3 system gets solved and the output resulting vector for the internal and input water fluxes is:

$$\bar{x} = \begin{bmatrix} Q_{FSGD} \\ Q_1 \\ Q_2 \end{bmatrix} = \begin{bmatrix} 662{,}842 \\ 5.804{,}242 \\ 5.169{,}103 \end{bmatrix} \quad [m^3/day]$$

Surprisingly, these results are the ones that are closer to the theoretical value (630 m3/day), resulting in an error of the 5%. This is an excellent level of accuracy, confirming the potential use

of this method. The final scheme with depicted fluxes between aquifer, the two boxes and the atmosphere are shown in Figure 27:

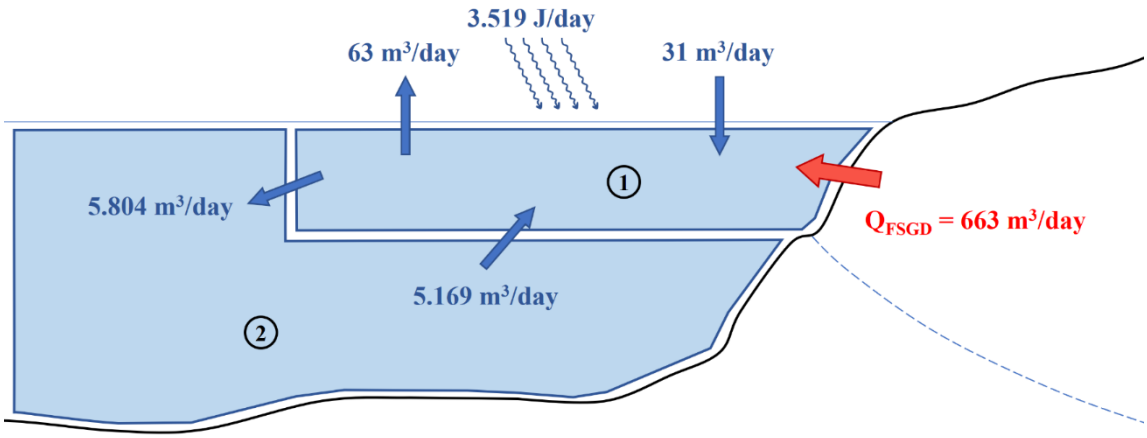

Figure 27. Solution to the box model 3x3 system in August campaign at Kahauloa Bay (Hawaii)

In the next chapter, results will be analyzed as a whole, and a final assessment of the methodologies tested in this study will be given. Reasons will be sought for both the accurate and the inaccurate values, to try to understand the reasons for the good and bad results.

6. DISCUSSION AND CONCLUSSIONS

At this point, a general analysis of the results should be made, being critical when evaluating the methodologies proposed. After having tested both the 'Submarine Outfalls' methodology and the 'Box Model' methodology in three different scenarios, the conclusions that can be drawn are the following:

1) In the process of methodology nº1, considering 'l' as the horizontal length of the plume implied disproportionate results, making it more than clear that this hypothesis must be taken as false.

   When considering that, values of 5 orders of magnitudes above the theoretical solution were obtained. This is probably due to the assumption we were forced to make in order to adapt the methodology to our real cases or scenarios. It was obvious that both hypotheses for the value of 'l' were far from each other and, therefore, would result in very different values of FSGD flows that would surely end up rejecting the veracity of one of them. A priori it was difficult to know which one would be the wrong consideration because both made sense to be applied for some reason.

2) When considering the other hypothesis, where 'l' is the vertical depth of the plume to the sea surface, the results improve but case after case the quality of the values obtained decreases.

   After the first hypothesis for 'l' value was rejected, the other one work quite good at the October's campaign in Castellón, with a 67% of accuracy with respect to the (García-Solsona et al., 2010) value. Those quite good results turned out to be a false perception because for the June's campaign at Torre Badum, accuracy level decreased until reaching an average value of 15-16% and, in contrast, in Hawaii's campaign the obtained values overpassed the 630 m^3/day being more than three times bigger on average. Even though, obtaining fluxes of the same order of magnitude is, without doubt, a good result.

   Thus, it is concluded that the submarine outfall methodology is not suitable to be applied in the resolution of these flow problems of an FSGD. It is evident from these results that none of the considerations taken for the adaptation of such a method is technically valid, as it distorts too much the conditions on which it is originally based. Forcing a variable to change its definition does not work and this is demonstrated by the values obtained.

3) As for methodology nº2, the complex box model option was discarded at the outset.

   Right on the first scenario in Torre Badum, this model 'broke down' for reasons that are not quite clear at this point. A possible reason for this situation may be the fact that in this 6x6 system of equations, the flow rates between boxes were considered only unidirectional, i.e. both the flow from box 1 into box 2 and the flow from box 2 to box 1 are merged into the same unknown and their direction depends on the sign.

From the very beginning, the direction of the flow was considered positive as it had more logic for the box model and, for algebraic reasons, the system was solved in such a way that the flows resulted in negative values, creating an incorrect balance in some state equations. For example, it can be seen how in the salinity balance equations it is not the same that in the product '$Q_{12}*S_1$' the flow rate turns out to be negative, as it would mean that water does not actually flow from box 1 to box 2 but vice versa. Instead of having in the system the term '$-Q_{12}*S_1$', the salinity would need to change and it should be '$Q_{21}*S_2$'. This problem does not happen in the simple variation of the model, were there is an unknown for the flux from box 1 to box 2, as well as an unknown for flux from box 2 to box 1.
The point here is that the complex model is not a proper methodology to use for FSGD flux estimation for obvious reasons.

4) Finally, opposed to the rest, the simple box model has been able to go through test after test, giving optimistic results for a possible development of this model.

   It is true that its accuracy level was not particularly outstanding at its first tests, with approximately a 30% of error in the both campaigns at Torre Badum (one by overestimation and the other by underestimation). Nevertheless, it is not a bad result as a first attempt for a methodology that has never been tested in a context such as this and which, if its evolution and development can improve its results, it could provide advantages over the system currently in use.
   Upon reaching the third scenario, the data improved and the value obtained with the Hawaii FSGD case was only 5% away from the value considered as a solution. This more than optimistic result means that the average balance of the overall project remains at an accuracy of 102%, i.e. with an excess flow of only 2%.

The application of only three scenarios does not give a reliable calibration system, but the numbers indicate a very promising potential. Indeed, one of the future options to keep improving the method would be to carry out many more scenarios to test until it is certain that the simple box model works for all types of SGD with a wide range of different conditions and properties.

It must be stated that with the obtained results, the study's expectations have been fulfilled since the objective was to find a methodology that had the potential to be used as a tool for flow estimation in submarine groundwater discharges. At no time was it required to achieve a very high percentage of accuracy, but the approximation of the results in the same order of magnitude. It was simply expected to achieve values similar to the ones estimated with natural tracers, since even the measurement techniques by Ra and Rn do not give results with negligible errors, as there is always a margin of error as in the García-Solsona et al., (2010) where margins of over 15% are given.

Obviously, the requirement of steady-state conditions is something that does not exactly happen in a real situation. These conditions (steady-state conditions: volume, salt and heat remain constants over period of time), in fact, are only met on few occasions because, by comparing salinity or temperature data through large periods of time, it can be seen how there

are significant differences form one time moment to another. As de Pedro, (2007) states: “The values obtained serve only to limit the order of magnitude of the flows while steady-state conditions last fulfilled, so the ‘Box Model’ methodology is limited to studies similar to the one presented here”.

As a general conclusion for this study, a new possibility is raised for the calculation of fresh groundwater fluxes discharged below sea level, offering advantages over the current measurements using radioactive Radium and Radon tracers. For example, both the in-situ measurement of Ra and Rn isotopes and its subsequent post-analysis in the laboratory by counting the isotopes with specialized machinery, are much more expensive and complex processes than standard measurements in oceanography such as data collection for temperature or salinity profiles (practically null, beyond the initial investment in thermal and conductivity sensors). As T and S data acquisition is also required in studies using radioactive isotope measurements, the economic cost of the new methodology would be significantly reduced, as well as the time required for the acquisition and post-processing of the necessary data.

It is true that current studies can also quantify the recirculated seawater to the coastal aquifer, which is also constituting part of the real discharge flux. Therefore, from an ocean point of view, the data obtained with the new method is partially 'incomplete', while from a strictly hydrogeological point of view it reveals very useful values to allow achieving mass balances in coastal aquifers, among many other uses.

Last but not least, returning to the economic issue, for many of the countries with lack of economic resources a relevant point is that the new method allows obtaining the values by means of a simple campaign for S and T data, being dispensable the monitoring network of piezometers in the lower part of the aquifer.

7. REFERENCES

Anderson, M.P., 2005. Heat as a ground water tracer. Ground Water, 43, 951–968.

Babenerd, B., 1991. Increasing oxygen deficiency in Kiel Bay (Western Baltic). A paradigm of progressing coastal eutrophication. *Meeresforsch,* 33 121-140.

Ballesteros, B.J., 1989. Estudio Hidrogeológico del Maestrazgo, Castellón, Instituto Geológico y minero de España documentation center, 158 pp.

Bejannin, S., San Beek, P., Stieglitz, T., Souhaut, M. and Tamborski, J., 2017. Combining airborne thermal infrared images and radium isotopes to study submarine groundwater discharge along the French Mediterranean coastline. Journal of Hydrology: Regional Studies, Volume 13, Pages 72-90. ISSN 2214-5818.

Brooks, N.H., 1973. Dispersion in Hydrologic and Coastal Environments. Environmental Protection Agency Rep. 660/3-73-010; also W. M. Keck, Laboratory Rep. KH-R-29, California Institute of Technology, Pasadena, California.

Burnett, W.C., Peterson, R., Moore, W.S. and De Oliveira, J., 2008. Radon and radium isotopes as tracers of submarine groundwater discharge — Results from the Ubatuba, Brazil SGD assessment intercomparison, Estuarine Coastal Shelf Sci., 76(3), 501 – 511.

Cameron, W.M. and Pritchard, D.W., 1963. Estuaries. In The Seas, Ideas and Observations on Progress in the Study of the Seas. Vol. 2, 306–324. Interscience Publ.

Capone, D. and Bautista, M., 1985. A groundwater source of nitrate in nearshore marine sediments. Nature 313, 214–216.

Cho, H.M., Kim, G., Kwon, E.Y., Moosdorf, N., García-Orellana, J. and Santos, I.R., 2018. Radium tracing nutrient inputs through submarine groundwater discharge in the global ocean. Sci Rep 8, 2439.

Climate Data: meteorological data at Torre Badúm (Castellón, Spain) and Kahauloa Bay (Big island of Hawaii, USA) for the campaigns dates. Data available at <climate-data.org>

Custodio, E., 2002. Coastal aquifers as important natural hydrogeological structures. Proceedings of the XXXII IAH and VI ALHSUD Congress Groundwater and Human Development, Mar del Plata, Italy, October 2002, pp 1905–1918.

De Pedro X., 2007. Situacions d'anòxia en zones estuàriques sense forçament mareal: una aproximació als balanços producció/consum d'oxigen. Ph.D. Thesis. Universitat de Barcelona, Spain.

Fischer, H.B., List, J., Koh, C., Imberger, J. And Brooks, N., 1979. Mixing in Inland and Coastal Waters. ISBN: 978-0-08-051177-1.

Flindt, M. R. and Kamp-Nielsen, L., 1997. Modelling of an estuarine eutrophication gradient. *EcologicalModelling,* 102 143-153.

Garcia-Solsona, E., Garcia-Orellana, J., Masqué, P. and Rodellas, V., Mejías, M., Ballesteros, B.J. and Domínguez, J.A., 2010. Groundwater and nutrient discharge through karstic coastal springs (Castelló, Spain). Biogeosciences 7, 2625–2638.

Hagy, J.D., Boynton, W.R. and Sanford, L.P., 2000. Estimation of net physical transport and hydraulic residence times for a coastal plain estuary using box models. Estuaries 23, 328–340.

Huyakorn, P.S., Andersen, P.F., Mercer, J.W. and White Jr., H.O., 1987. Saltwater intrusion in aquifers: Development and testing of a three-dimensional finite element model. Water Resources Research, 23(2), 293-312.

IOC-UNESCO and UNEP, 2016. Large Marine Ecosystems: Status and Trends. In: Transboundary Waters Assessment Programme. Vol. 4. Nairobi: United Nations Environment Programme (UNEP). isbn: 9782831711577.

Jiao, J. and Post, V., 2019. Coastal Hydrogeology. I. Cambridge University Press. isbn: 9781139344142.

Johnson, A.G., Glenn, C.R., Burnett, W.C., Peterson, R.N. and Lucey, P.G., 2008. Aerial infrared imaging reveals large nutrient-rich groundwater inputs to the ocean. Geophysical Research Letters 35, L15606.

Justic, D., Rabalais, N.N. and Turner, R.E., 1997. Impacts of climate change on net productivity of coastal waters: Implications forcarbon budgets and hypoxia. *Climate Research,* 8 (3): 225-237.

Kalakan, C. and Motz, L.H., 2018. Saltwater Intrusion and Recirculation of Seawater in Isotropic and Anisotropic Coastal Aquifers. Journal of Hydrologic Engineering, vol. 23, issue 11 (November 2018).

Kelly, J.L., Glenn, C.R. and Lucey, P.G., 2013. High-resolution aerial infrared mapping of groundwater discharge to the coastal ocean. Limnol. Oceanogr.: Methods 11: 262– 277.

Kumar, M., Ramanathan, A.L., Neupane, B.R., Van Tu, D. and Kim, S., 2010. Critical Evaluation of the Recent Development and Trends in Submarine Groundwater Discharge Research in Asia. Management and Sustainable Development of Coastal Zone Environments. ISBN: 978-90-481-3067-2.

Linacre, E.T., 1977. A simple formula for estimating evaporation rates in various climates using temperature alone. Agricultural Meteorology, Amsterdam, v. 18.

Matsukawa, Y. and Sasaki, K., 1990. Nitrogen budget in Tokyo Bay with special reference to the low sedimentation to supply ratio. Journal of the Oceanographical Society of Japan 46, 44–54.

Mejías, M., García-Orellana, J., Plata, J.L., Marina, M., García-Solsona, E., Ballesteros, B., Masqué, P., López, J. and Fernández-Arrojo, C., 2008. Methodology of hydrogeological characterization of deep carbonate aquifers as potential reservoirs of groundwater. Case of study: the Jurassic aquifer of El Maestrazgo (Castellón, Spain). Environ Geol 54, 521–536.

Mejías, M., Ballesteros, B.J., Anton-Pacheco, C., Domínguez, J.A., García-Orellana, J., García-Solsona, E. and Masqué, P., 2012. Methodological study of submarine groundwater discharge from a karstic aquifer in the Western Mediterranean Sea. Journal of Hydrology, 464, 27–40.

Michael, H.A., Post, V.E.A., Wilson, A.M. and Werner, A.D., 2017. Science, society, and the coastal groundwater squeeze. In: Water Resources Research 53.4, pp. 2610–2617. issn: 00431397.

Moore, W.S., 1999. The subterranean estuary: A reaction zone of groundwater and sea water. Mar. Chem. 65:111-126.

Moore, W.S., 2000. Ages of continental shelf waters determined from Ra-223 and Ra- 224. Journal of Geophysical Research, Oceans, 105, 22117–22122.

Moore, W.S., 2010. The Effect of Submarine Groundwater Discharge on the Ocean. In: Annual Review of Marine Science 2.1, pp. 59–88. issn: 1941-1405.

Munekage, Y. and Kimura, H., 1985. On the exchange of sea water in the lower layer of Uranouchi Bayby the box-model method. *Rep. USA Mar. Biol. Inst. Kochi Univ. Kochidai Kaiyoseibutsukenho,* 7 61-72.

Norro, A. and Frankignoulle, M., 1996. Biogeochemical box modelling at small scale application to the inorganic carbon cycle in the Bay of Calvi. *Ecological Modelling,* 88 101-112.

Officer, C.B., 1976. Physical oceanography of estuaries and associated coastal waters: 465. John Wiley and Sond, Inc., New York.

Officer, C.B., 1983. Physics of estarine circulation. In: *Estuaries and enclosed seas*, 26, 15-41. Elsevier, Amsterdam.

Padilla, F., Méndez, A., Fernández, R. and Vellando, P. R., 2008. Numerical modelling of surfacewater/groundwater flows for freshwater/saltwater hydrology: the case of the alluvial coastal aquifer of the Low Guadalhorce River, Malaga, Spain. Environ Geol 55, 215–226.

Penman, H. L., 1948. Natural evaporation from open water, bare soil and grass. *Proc. Roy. Soc. London*, A193 120-146.

Peterson, R., Burnett, W.C., Glenn, C.R. and Johnson, A.G., 2009. Quantification of point-source groundwater discharges to the ocean from the shoreline of the big island, Hawaii. Limnology and Oceanography, 54, 890–904.

Pinet, P. R., 2013. Invitation to Oceanography, Jones & Bartlett Learning. ISBN:978-1-4496-4802-2

Pool, M. and Carrera, J., 2010. Dynamics of negative hydraulic barriers to prevent seawater intrusion. Hydrogeology journal, 18(1), 95-105.

Post, V.E.A., 2005. Fresh and saline groundwater interaction in coastal aquifers: Is our technology ready for the problems ahead?. *Hydrogeology Journal*, 13(1), 120-123.

Pritchard, D.W., 1952. Estuarine Hydrography. Advances in Geophysics, Volume 1. Edited by H. E. Landsberg, Geophysics Research Directorate, Air Force Cambrigde Research Center. Published by Academic Press, Inc., New York, USA, 1952, p.243.

Rattray, M. Jr. and Hansen, D.V., 1962. A similarity solution for circulation in an estuary. *J. Mar. Res.* 20, 121-133.

Sharqawy, M.H. and Zubair, S.M., 2010. Thermophysical properties of seawater: a review of existing correlations and data. Desalination Water Treat. 16.

Smith, A.J., Turner, J.V., Herne, D.E. and Hick, W.P., 2003. Quantifying submarine groundwater discharge and nutrient discharge into Cockburn Sound Western Australia, Final Technical Report to Coast and Clean Seas — Natural Heritage Trust. Project WA9911: CSIRO Land and Water Consultancy Report No 1/03, 210 pp.

Suzuki, T. and Matsukawa, Y., 1987. Hydrography and budget of dissolved total nitrogen and dissolvedoxygen in the stratified season in Mikawa Bay, Japan. *J. Oceanogr. Soc. Japan,* 43 (1): 37-48.

Taniguchi, M., Dulai, H., Burnett, K.M., Santos, I.R., Sugimoto, R., Stieglitz, T., Kim, G., Moosdorf, N. and Burnett, W.C., 2019. Submarine Groundwater Discharge: Updates on Its Measurement Techniques, Geophysical Drivers, Magnitudes, and Effects. In: Frontiers in Environmental Science 7. October, pp. 1–26. issn: 2296665X.

Todd, D.K., 1959. Groundwater hydrology. John Wily & Sons, Inc., New York.

Tomczak, M., 1996. Oceanography Lecture Notes, Lecture 12: Estuaries. Data available at <http://www.mt-oceanography.info/IntroOc/lecture12.html>

UNESCO, 1981a. Escala práctica de salinidad 1978 y la Ecuación Internacional de estado del agua de mar 1980. Tech. Pap. Mar. Sci., 36: 25 pp.

UNESCO, 2004. Submarine groundwater discharge: management implications, measurements and effects. IHP-VI series on groundwater; IOC. Manuals and guides, vol 5(44).

Varela, R.A. and Rosón Porto, G., 2008. Métodos en Oceanografía Física. Editorial Anthias. ISBN : 978-84-933167-4-7

Varma, S., Turner, J.V. and Underschultz, J., 2010. Estimation of submarine groundwater discharge into Geographe Bay, Bunbury, Western Australia. J. Geochem. Expl. 106, 197–210.

Werner, A.D., Bakker, M., Post, V.E.A., Vandenbohede, A., Lu, C., Ataie-Ashtiani, B., Simmons, C.T. and Barry, D.A., 2013. Seawater intrusion processes, investigation and management: recent advances and future challenges. Advances in Water Resources, 51, 3-26.